

*J*

AFOSR - TR - 76 - 1080

12

DYNAMIC ANALYSIS OF A LOADED CONICAL ANTENNA  
OVER A GROUND PLANE

Donald R. Wilton

Prepared by

Department of Electrical Engineering  
University of Mississippi  
University, MS 38677

for

Air Force Office of Scientific Research  
Bolling Air Force, D.C. 20332

Grant No. AFOSR 75-2832

August 1976

Approved for public release;  
distribution unlimited.

*J*

D D C  
RECEIVED  
DEC 9 1976

Reproduced From  
Best Available Copy

AIR FORCE OFFICE OF SCIENTIFIC RESEARCH (AFSC)  
NOTICE OF TRANSMITTAL TO DDC  
This technical report has been reviewed and is  
approved for public release IAW AFR 190-12 (7b).  
Distribution is unlimited.  
A. D. BLOOM  
Technical Information Officer

UNCLASSIFIED

SECURITY CLASSIFICATION OF THIS PAGE (When Data Entered)

19 REPORT DOCUMENTATION PAGE		READ INSTRUCTIONS BEFORE COMPLETING FORM	
1. REPORT NUMBER	2. GOVT ACCESSION NO.	3. RECIPIENT'S CATALOG NUMBER	
18 AFOSR - (TR-76-1080) ✓			
4. TITLE (and Subtitle)		5. TYPE OF REPORT & PERIOD COVERED	
6 DYNAMIC ANALYSIS OF A LOADED CONICAL ANTENNA OVER A GROUND PLANE.		9 Final - Pt II	
7. AUTHOR(s)		6. PERFORMING ORG. REPORT NUMBER	
10 Donald R. Wilton			
8. CONTRACT OR GRANT NUMBER(s)		15 YAF - AFOSR 2832-75	
9. PERFORMING ORGANIZATION NAME AND ADDRESS		10. PROGRAM ELEMENT, PROJECT, TASK AREA & WORK UNIT NUMBERS	
Department of Electrical Engineering University of Mississippi University, MS 38677		61102F 16 975135 17 05	
11. CONTROLLING OFFICE NAME AND ADDRESS		12. REPORT DATE	
Air Force Office of Scientific Research /NP Bolling Air Force Base, D.C. 20332		11 Aug 1976	
13. MONITORING AGENCY NAME & ADDRESS (if different from Controlling Office)		13. NUMBER OF PAGES	
12 88p.		86	
14. DISTRIBUTION STATEMENT (of this Report)		15. SECURITY CLASS. (of this report)	
Approved for Public Release: Distribution Unlimited		UNCLASSIFIED	
15a. DECLASSIFICATION/DOWNGRADING SCHEDULE			
16. DISTRIBUTION STATEMENT (of the abstract entered in Block 20, if different from Report)			
17. SUPPLEMENTARY NOTES			
TECH OTHER			
18. KEY WORDS (Continue on reverse side if necessary and identify by block number)			
EMP SIMULATOR, BICONICAL ANTENNA, INTEGRAL EQUATION, IMPEDANCE LOADING			
19. ABSTRACT (Continue on reverse side if necessary and identify by block number)			
Integral equations are derived and solved numerically for the current distribution on a resistively loaded conical antenna over a ground plane. Representative current distributions, input impedance values, and radiation patterns are given for the loaded and unloaded structure with and without a topcap.			

Reproduced From  
Best Available Copy

DYNAMIC ANALYSIS OF A LOADED CONICAL ANTENNA  
OVER A GROUND PLANE

by

Donald R. Wilton

Department of Electrical Engineering  
University of Mississippi  
University, MS 38677

for

Air Force Office of Scientific Research  
Bolling Air Force, D.C. 20332

Grant No. AFOSR 75-2832

August 1976

Approved for public release;  
distribution unlimited.

Reproduced From  
Best Available Copy

### ABSTRACT

Three integral equations are derived and formulated for numerical solution for the currents induced on a resistively loaded conical antenna over a ground plane. The first integral equation is a relatively simple one for a cone without a topcap. The second and third integral equations are applicable to a cone with or without a topcap, but the latter equation is relatively cumbersome, involving complicated kernels with various singularities. A computer code has been developed for each of the three methods. Numerical data for current distributions, input impedances and radiation patterns are presented for resistively loaded and unloaded structures, both with and without topcap.

White Sheet of	✓
Paper 1104	11
1105	11
1106	11
1107	11
1108	11
1109	11
1110	11
1111	11
1112	11
1113	11
1114	11
1115	11
1116	11
1117	11
1118	11
1119	11
1120	11
1121	11
1122	11
1123	11
1124	11
1125	11
1126	11
1127	11
1128	11
1129	11
1130	11
1131	11
1132	11
1133	11
1134	11
1135	11
1136	11
1137	11
1138	11
1139	11
1140	11
1141	11
1142	11
1143	11
1144	11
1145	11
1146	11
1147	11
1148	11
1149	11
1150	11
1151	11
1152	11
1153	11
1154	11
1155	11
1156	11
1157	11
1158	11
1159	11
1160	11
1161	11
1162	11
1163	11
1164	11
1165	11
1166	11
1167	11
1168	11
1169	11
1170	11
1171	11
1172	11
1173	11
1174	11
1175	11
1176	11
1177	11
1178	11
1179	11
1180	11
1181	11
1182	11
1183	11
1184	11
1185	11
1186	11
1187	11
1188	11
1189	11
1190	11
1191	11
1192	11
1193	11
1194	11
1195	11
1196	11
1197	11
1198	11
1199	11
1200	11
1201	11
1202	11
1203	11
1204	11
1205	11
1206	11
1207	11
1208	11
1209	11
1210	11
1211	11
1212	11
1213	11
1214	11
1215	11
1216	11
1217	11
1218	11
1219	11
1220	11
1221	11
1222	11
1223	11
1224	11
1225	11
1226	11
1227	11
1228	11
1229	11
1230	11
1231	11
1232	11
1233	11
1234	11
1235	11
1236	11
1237	11
1238	11
1239	11
1240	11
1241	11
1242	11
1243	11
1244	11
1245	11
1246	11
1247	11
1248	11
1249	11
1250	11
1251	11
1252	11
1253	11
1254	11
1255	11
1256	11
1257	11
1258	11
1259	11
1260	11
1261	11
1262	11
1263	11
1264	11
1265	11
1266	11
1267	11
1268	11
1269	11
1270	11
1271	11
1272	11
1273	11
1274	11
1275	11
1276	11
1277	11
1278	11
1279	11
1280	11
1281	11
1282	11
1283	11
1284	11
1285	11
1286	11
1287	11
1288	11
1289	11
1290	11
1291	11
1292	11
1293	11
1294	11
1295	11
1296	11
1297	11
1298	11
1299	11
1300	11
1301	11
1302	11
1303	11
1304	11
1305	11
1306	11
1307	11
1308	11
1309	11
1310	11
1311	11
1312	11
1313	11
1314	11
1315	11
1316	11
1317	11
1318	11
1319	11
1320	11
1321	11
1322	11
1323	11
1324	11
1325	11
1326	11
1327	11
1328	11
1329	11
1330	11
1331	11
1332	11
1333	11
1334	11
1335	11
1336	11
1337	11
1338	11
1339	11
1340	11
1341	11
1342	11
1343	11
1344	11
1345	11
1346	11
1347	11
1348	11
1349	11
1350	11
1351	11
1352	11
1353	11
1354	11
1355	11
1356	11
1357	11
1358	11
1359	11
1360	11
1361	11
1362	11
1363	11
1364	11
1365	11
1366	11
1367	11
1368	11
1369	11
1370	11
1371	11
1372	11
1373	11
1374	11
1375	11
1376	11
1377	11
1378	11
1379	11
1380	11
1381	11
1382	11
1383	11
1384	11
1385	11
1386	11
1387	11
1388	11
1389	11
1390	11
1391	11
1392	11
1393	11
1394	11
1395	11
1396	11
1397	11
1398	11
1399	11
1400	11
1401	11
1402	11
1403	11
1404	11
1405	11
1406	11
1407	11
1408	11
1409	11
1410	11
1411	11
1412	11
1413	11
1414	11
1415	11
1416	11
1417	11
1418	11
1419	11
1420	11
1421	11
1422	11
1423	11
1424	11
1425	11
1426	11
1427	11
1428	11
1429	11
1430	11
1431	11
1432	11
1433	11
1434	11
1435	11
1436	11
1437	11
1438	11
1439	11
1440	11
1441	11
1442	11
1443	11
1444	11
1445	11
1446	11
1447	11
1448	11
1449	11
1450	11
1451	11
1452	11
1453	11
1454	11
1455	11
1456	11
1457	11
1458	11
1459	11
1460	11
1461	11
1462	11
1463	11
1464	11
1465	11
1466	11
1467	11
1468	11
1469	11
1470	11
1471	11
1472	11
1473	11
1474	11
1475	11
1476	11
1477	11
1478	11
1479	11
1480	11
1481	11
1482	11
1483	11
1484	11
1485	11
1486	11
1487	11
1488	11
1489	11
1490	11
1491	11
1492	11
1493	11
1494	11
1495	11
1496	11
1497	11
1498	11
1499	11
1500	11
1501	11
1502	11
1503	11
1504	11
1505	11
1506	11
1507	11
1508	11
1509	11
1510	11
1511	11
1512	11
1513	11
1514	11
1515	11
1516	11
1517	11
1518	11
1519	11
1520	11
1521	11
1522	11
1523	11
1524	11
1525	11
1526	11
1527	11
1528	11
1529	11
1530	11
1531	11
1532	11
1533	11
1534	11
1535	11
1536	11
1537	11
1538	11
1539	11
1540	11
1541	11
1542	11
1543	11
1544	11
1545	11
1546	11
1547	11
1548	11
1549	11
1550	11
1551	11
1552	11
1553	11
1554	11
1555	11
1556	11
1557	11
1558	11
1559	11
1560	11
1561	11
1562	11
1563	11
1564	11
1565	11
1566	11
1567	11
1568	11
1569	11
1570	11
1571	11
1572	11
1573	11
1574	11
1575	11
1576	11
1577	11
1578	11
1579	11
1580	11
1581	11
1582	11
1583	11
1584	11
1585	11
1586	11
1587	11
1588	11
1589	11
1590	11
1591	11
1592	11
1593	11
1594	11
1595	11
1596	11
1597	11
1598	11
1599	11
1600	11
1601	11
1602	11
1603	11
1604	11
1605	11
1606	11
1607	11
1608	11
1609	11
1610	11
1611	11
1612	11
1613	11
1614	11
1615	11
1616	11
1617	11
1618	11
1619	11
1620	11
1621	11
1622	11
1623	11
1624	11
1625	11
1626	11
1627	11
1628	11
1629	11
1630	11
1631	11
1632	11
1633	11
1634	11
1635	11
1636	11
1637	11
1638	11
1639	11
1640	11
1641	11
1642	11
1643	11
1644	11
1645	11
1646	11
1647	11
1648	11
1649	11
1650	11
1651	11
1652	11
1653	11
1654	11
1655	11
1656	11
1657	11
1658	11
1659	11
1660	11
1661	11
1662	11
1663	11
1664	11
1665	11
1666	11
1667	11
1668	11
1669	11
1670	11
1671	11
1672	11
1673	11
1674	11
1675	11
1676	11
1677	11
1678	11
1679	11
1680	11
1681	11
1682	11
1683	11
1684	11
1685	11
1686	11
1687	11
1688	11
1689	11
1690	11
1691	11
1692	11
1693	11
1694	11
1695	11
1696	11
1697	11
1698	11
1699	11
1700	11
1701	11
1702	11
1703	11
1704	11
1705	11
1706	11
1707	11
1708	11
1709	11
1710	11

## SECTION I

### INTRODUCTION

In a companion report [1], the static analysis of a conical antenna over a ground plane is presented. In this report, the analysis is extended to treat the time-harmonic case and to incorporate a model of the resistive loading of the structure. The resistive loading is intended to reduce the effect of diffraction from the cone edge at the higher frequencies.

If the cone has no topcap, the analysis may be considerably simplified and a simple integral equation for this situation is derived in Section II and implementation of a moment method solution is considered in Section III. In Section IV, an integral equation for the cone with a topcap is derived. Presented in Section V are numerical results in the frequency domain currents for a loaded conical antenna both with and without a topcap. In Appendix A expressions are derived for the computation of fields from the currents and Appendix B gives the derivation of an alternate integral equation from that derived in Section IV.

SECTION II  
FORMULATION OF AN INTEGRAL EQUATION FOR  
A BICONE WITHOUT ENDCAPS

For the symmetrically driven biconical structure of Figure 1, the current on both the cone and its image are radially directed and have no circumferential ( $\phi$ ) variation. Hence the magnetic field tangent to the cone is  $\phi$ -directed and the boundary conditions can be satisfied by fields which are transverse magnetic (TM) to  $r$ . Thus, the fields may be completely determined by a radially-directed vector potential  $\bar{A} = A_r \hat{r}$  [2]. In an eigenfunction solution to such problems, the fields are determined in the bicone region from a vector potential  $A_r$  which comes from a homogeneous solution of the wave equation. In order to derive an integral equation, however,  $A_r$  must be expressed in terms of the current on the bicone. In particular, a free space Green's function is to be found for the vector potential  $A_r$  due to a unit radially-directed current element. A superposition integral then expresses the total vector potential due to currents on the cone.

Beginning with the assumption that the magnetic field is determined from  $\bar{A} = A_r \hat{r}$ ,

$$\bar{H} = \frac{1}{\mu} \nabla \times \bar{A}$$

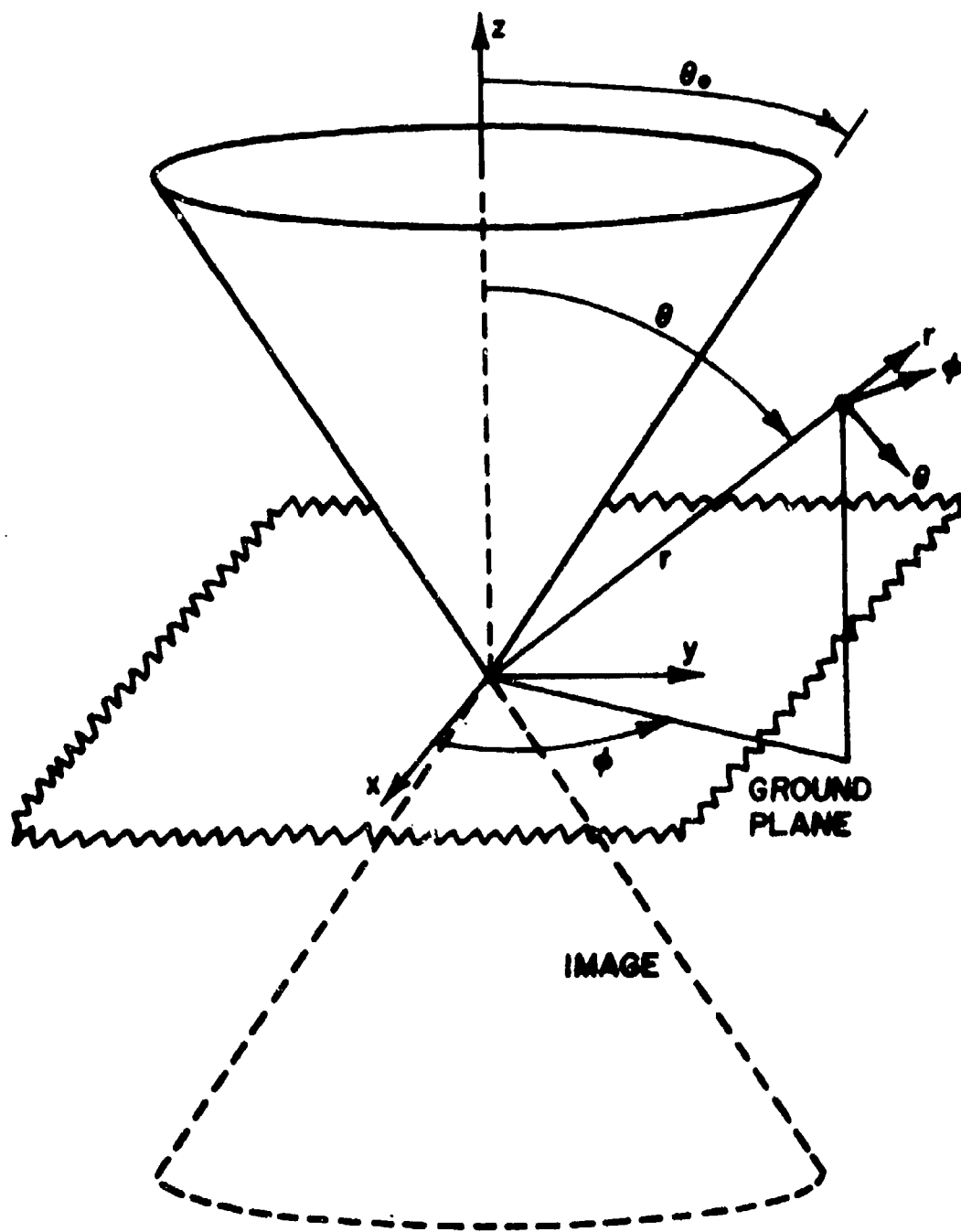


Figure 1. Geometry of cone over a ground plane.



and using Maxwell's equations,

$$\nabla \times \vec{E} = -j\omega\mu\vec{H}$$

$$\nabla \times \vec{H} = j\omega\epsilon\vec{E} + \vec{J}$$

one readily determines by standard procedures, that  $\vec{A}$  satisfies the vector Helmholtz equation

$$\nabla \times \nabla \times \vec{A} - k^2 \vec{A} = \mu \vec{J}_r \hat{r} - j\omega\mu\epsilon \nabla \phi \quad (1)$$

where  $\phi$  is a scalar such that

$$\vec{E} = -j\omega\vec{A} - \nabla\phi$$

For a radially-directed unit current element,

$$\begin{aligned} \vec{J} &= J_r \hat{r} = \rho \delta(\vec{r} - \vec{r}') \\ &= \hat{r} \frac{\delta(r-r') \delta(\theta-\theta') \delta(\phi-\phi')}{r'^2 \sin^2 \theta'} \end{aligned} \quad (2)$$

Expanding out (1) yields

$$\begin{aligned} &\left[ \frac{-1}{r^2 \sin \theta} \frac{\partial}{\partial \theta} \left( \sin \theta \frac{\partial A_r}{\partial \theta} \right) - \frac{1}{r^2 \sin^2 \theta} \frac{\partial^2 A_r}{\partial \phi^2} - k^2 A_r \right] \hat{r} \\ &+ \left( \frac{1}{r} \frac{\partial^2 A_r}{\partial r \partial \theta} \right) \hat{\theta} + \left( \frac{1}{r \sin \theta} \frac{\partial^2 A_r}{\partial \phi \partial r} \right) \hat{\phi} \\ &= \mu J_r \hat{r} - j\omega\mu\epsilon \left( \frac{\partial \phi}{\partial r} \hat{r} + \frac{1}{r} \frac{\partial \phi}{\partial \theta} \hat{\theta} + \frac{1}{r \sin \theta} \frac{\partial \phi}{\partial \phi} \hat{\phi} \right) \end{aligned} \quad (3)$$

from which it is seen that

$$\begin{aligned}\frac{\partial^2 A_r}{\partial r \partial \theta} &= -j\omega\mu\epsilon \frac{\partial \phi}{\partial \theta} \\ \frac{\partial^2 A_r}{\partial \phi \partial r} &= -j\omega\mu\epsilon \frac{\partial \phi}{\partial \phi}\end{aligned}\quad (4)$$

These conditions are automatically satisfied by the gauge choice

$$\phi = -\frac{1}{j\omega\mu\epsilon} \frac{\partial A_r}{\partial r} \quad (5)$$

Substituting (2) and (5) into (3) leaves the one scalar component equality

$$\begin{aligned}\frac{\partial^2 A_r}{\partial r^2} + \frac{1}{r^2 \sin \theta} \frac{\partial}{\partial \theta} \left( \sin \theta \frac{\partial A_r}{\partial \theta} \right) + \frac{1}{r^2 \sin \theta} \frac{\partial^2 A_r}{\partial \phi^2} \\ + k^2 A_r = -\mu \delta(\vec{r} - \vec{r}')\end{aligned}\quad (6)$$

which can be rewritten in the more convenient form,

$$(\nabla^2 + k^2) \left( \frac{A_r}{r} \right) = \frac{-\mu \delta(\vec{r} - \vec{r}')}{r'} \quad (7)$$

To obtain (7), one notes that

$$\frac{\delta(\vec{r} - \vec{r}')}{r} = \frac{\delta(\vec{r} - \vec{r}')}{r'}$$

A solution of (7) which satisfies the radiation condition for a  $\exp(j\omega t)$  time convention may be written by inspection of (7) as

$$A_r = \frac{\mu r}{4\pi r'} \frac{e^{-jk|\bar{r}-\bar{r}'|}}{|\bar{r}-\bar{r}'|} \quad (8)$$

and the general solution to (3) for a distributed set of currents is obtained by superposition:

$$A_r = \frac{\mu}{4\pi} \int_V J_r(\bar{r}') \frac{r e^{-jk|\bar{r}-\bar{r}'|}}{r' |\bar{r}-\bar{r}'|} dv' \quad (9)$$

This form of the vector potential has also been used by others [3]. For the symmetrically-excited cone and its image,

$$J_r(\bar{r}') = \frac{J_{sr}(\bar{r}')}{r'} \left[ \delta(\theta' - \theta_0) - \delta(\theta' - \pi + \theta_0) \right] \quad (10)$$

where  $J_{sr}$  is the bicone surface current density. Substituting (10) into (9) gives the desired equation for the vector potential:

$$A_r = \frac{\mu r \sin \theta_0}{4\pi} \int_0^{2\pi} \int_0^L J_{sr}(r') \left( \frac{e^{-jkR^+}}{R^+} - \frac{e^{-jkR^-}}{R^-} \right) dr' d\phi' \quad (11)$$

where

$$R^\pm = \sqrt{r^2 + r'^2 - 2rr'[\sin \theta \sin \theta_0 \cos(\phi - \phi') \pm \cos \theta \cos \theta_0]}$$

The plus superscript denotes source points on the upper bicone surface while the negative sign denotes source points on the image surface.

It is convenient to introduce the total axial current

$$I(r') = 2\pi r' \sin \theta_0 J_{sr}(r') \quad (12)$$

so that (11) becomes

$$A_r = -\frac{\mu r}{8\pi^2} \int_0^{2\pi} \int_0^L \frac{I(r')}{r'} \left[ \frac{e^{-jkR^+}}{R^+} - \frac{e^{-jkR^-}}{R^-} \right] dr' d\phi' \quad (13)$$

The radial component of electric field is now given by

$$E_r = \frac{1}{j\omega\mu\epsilon} \left( \frac{\partial^2}{\partial r^2} + k^2 \right) A_r \quad (14)$$

The simplicity of (13) and (14) compared to the usual vector potential representations should be emphasized at this point. One notes that in the usual representation, two vector potential components,  $A_r$  and  $A_\theta$ , would be present. Furthermore, the integrands of the potential integrals would contain somewhat complicated dependences on angles between observation and source points which arise from projecting the source vector onto the potential component vector for each source and observation point. Finally, the expression for the radially-directed electric field would be complicated and difficult to handle numerically compared to the approach to be followed here. These complications indeed will appear in the formulation which includes a topcap on the bicone structure (Appendix B).

An integral equation for the current is obtained by applying the boundary condition that the radial electric field must equal the impedance loading times the total current density, i.e.,

$$E_r = Z_s(r)I(r)$$

Since all currents and fields are  $\phi$ -independent, it suffices to take all observation points along the intersection of the plane  $\phi=0$  and the conical surface. Hence, we obtain finally

$$\frac{1}{j\omega\mu\epsilon} \left[ \frac{d^2}{dr^2} + k^2 \right] A_r - Z_s(r)I(r) = 0, \quad 0 < r \leq l, \quad \theta = \theta_0, \phi = 0 \quad (15)$$

Equation (15) is an integro-differential equation for the induced current on the bicone. As it stands, (15) does not appear to contain a driving term due to the applied voltage at the bicone terminals. In the next section, however, this term appears as a "boundary" condition on  $dA_r/dr$  at  $r=0$ . One also notes in (15) that discrete or lumped loading may be introduced by allowing  $Z_s(r)$  to be represented by appropriate  $\delta$ -functions,

$$Z_s(r) = \sum_{n=1}^{N_L} Z_{Ln} \delta(r-r_{Ln})$$

for  $N_L$  loads where  $Z_{Ln}$  is the impedance of the  $n^{\text{th}}$  load located at  $r=r_{Ln}$ .

### SECTION III

#### APPLICATION OF METHOD OF MOMENTS TO A BICONE WITHOUT ENDCAPS

The usual procedure in applying the method of moments [4] is to first represent the unknown current as a linear combination of an appropriate set of basis functions and then "test" the resulting integral equation with a series of testing functions. Here it is convenient to reverse this order and to first test the equation before expanding the current. A set of testing functions which offer a number of advantages in a numerical procedure are the piecewise sinusoidal testing functions:

$$w_1(r) = \begin{cases} \frac{\sin k(\Delta r - r)}{\sin k\Delta r} & , \quad 0 \leq r \leq \Delta r \\ 0 & , \quad \Delta r \leq r \leq L \end{cases}$$

$$w_m(r) = \begin{cases} \frac{\sin k(\Delta r - |r - r_m|)}{\sin k\Delta r} & , \quad r_{m-1} \leq r \leq r_{m+1} \\ 0 & , \quad |r - r_m| > \Delta r \end{cases}$$

$m = 2, 3, \dots, M \quad (16)$

where  $\Delta r = L/M$ ,  $r_m = (m-1)\Delta r$ ,  $m=1, 2, \dots, M$ .

These testing functions are shown in Figure 2. An inner product is next defined as

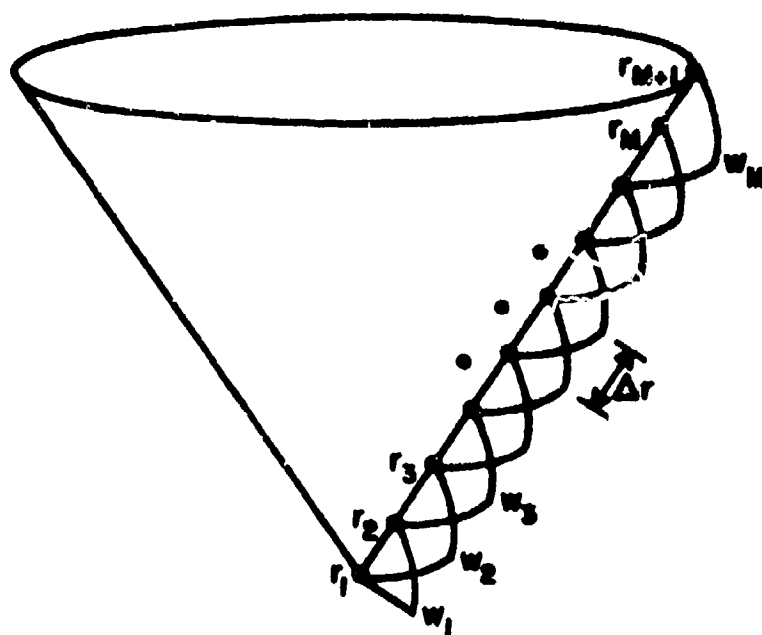


Figure 2. Testing functions for the cone.

$$\langle f(r), g(r) \rangle = \int_0^L f(r)g(r)dr \quad (17)$$

and (15) is successively tested with each of the  $w_m$ ,  
 $m=1,2,\dots,M$ :

$$\frac{1}{j\omega\mu\epsilon} \left\langle \left( \frac{d^2}{dr^2} + k^2 \right) A_r, w_m \right\rangle - \langle z_s(r)I(r), w_m \rangle = 0, \quad m=1,2,\dots,M \quad (18)$$

Taking, for the moment,  $m=1$  and integrating the first term by parts twice results in

$$\left\langle \left( \frac{d^2}{dr^2} + k^2 \right) A_r, w_1 \right\rangle = - \left. \frac{dA_r}{dr} \right|_{r=0} + \frac{k}{\sin k\Delta r} A_r(r_2) - \frac{k \cos k\Delta r}{\sin k\Delta r} A_r(r_2)$$

where  $A_r(r_m) = A_r \Big|_{r=r_m}$ . Note that although

$$A_r \Big|_{\theta=\pi/2} = 0, \quad (19)$$

$A_r(r_1)$  is not zero along the bicone. In fact, one notes that

$$E_\theta = \frac{1}{j\omega\mu\epsilon r} \frac{\partial^2 A_r}{\partial r \partial \theta}$$

and that the bicone voltage at  $r=0$  is just



$$\begin{aligned}
 V_0 &= \int_{\theta_0}^{\pi/2} E_{\theta} r d\theta \Big|_{r=0} \\
 &= \frac{1}{j\omega\mu\epsilon} \int_{\theta_0}^{\pi/2} \frac{\partial^2 A_r}{\partial r \partial \theta} d\theta \Big|_{r=0} = - \frac{1}{j\omega\mu\epsilon} \frac{\partial A_r(r_1)}{\partial r}
 \end{aligned}$$

where, using (19), one sees that  $\partial A_r / \partial r = 0$  at  $\theta = \pi/2$ .

Thus for  $m=1$ , (18) becomes

$$\begin{aligned}
 \frac{k}{j\omega\mu\epsilon \sin k\Delta r} \left[ -\cos k\Delta r A_r(r_1) + A_r(r_2) \right] \\
 - \left\langle Z_s(r) I(r), w_1 \right\rangle = -V_0 \quad (20)
 \end{aligned}$$

For  $m = 2, 3, 4, \dots, M$ , integration by parts twice in (18) results in

$$\begin{aligned}
 \frac{k}{j\omega\mu\epsilon \sin k\Delta r} \left[ A_r(r_{m+1}) - 2 \cos k\Delta r A_r(r_m) + A_r(r_{m-1}) \right] \\
 - \left\langle Z_s(r) I(r), w_m \right\rangle = 0
 \end{aligned}$$

$$m = 2, 3, \dots, M \quad (21)$$

Note that the choice of testing functions has resulted in removing all the derivative operations from the operator equations. This is the principal advantage of the testing functions chosen.

A matrix equation now results if the current is expanded in an appropriate set of basis functions. A convenient set is the pulse functions defined by

$$p_1(r) = \begin{cases} 1, & 0 \leq r \leq \Delta r/2 \\ 0, & \Delta r/2 \leq r \leq L \end{cases}$$

$$p_n(r) = \begin{cases} 1, & |r - r_n| \leq \Delta r/2 \\ 0, & |r - r_n| > \Delta r/2 \end{cases}$$

$$n = 2, 3, \dots, M$$

(see Figure 3) and the resulting current expansion is

$$I(r) \approx \sum_{n=1}^M I_n p_n(r) \quad (22)$$

Note that the current at the bicone edge  $r=L$  is automatically zero by our choice of basis functions (Figure 3).

When (22) is substituted into (20) and (21), there results the system of linear equations

$$I_1 \left\{ \frac{k}{j\omega\mu\epsilon \sin k\Delta r} \left[ -\cos k\Delta r \Psi(r_1; r_1, r_{1+}) + \Psi(r_2; r_2, r_{1+}) \right] - \left\langle Z_s(r) p_1(r), w_1 \right\rangle \right\} +$$

$$\begin{aligned}
& + \sum_{n=2}^M I_n \left\{ \frac{k}{j\omega\mu\epsilon \sin k\Delta r} \left[ -\cos k\Delta r \Psi(r_1; r_{n-}, r_{n+}) + \Psi(r_2; r_{n-}, r_{n+}) \right] \right. \\
& \quad \left. - \langle Z_s(r) p_n(r), w_1 \rangle \right\} = -V_0
\end{aligned}
\tag{23}$$

and

$$\begin{aligned}
& I_1 \left\{ \frac{k}{j\omega\mu\epsilon \sin k\Delta r} \left[ \Psi(r_{m-1}; r_1, r_{1+}) - 2 \cos k\Delta r \Psi(r_m; r_1, r_2) \right. \right. \\
& \quad \left. \left. + \Psi(r_{m+1}; r_1, r_{1+}) \right] - \langle Z_s(r) p_1(r), w_m \rangle \right\} \\
& + \sum_{n=2}^M I_n \left\{ \frac{k}{j\omega\mu\epsilon \sin k\Delta r} \left[ \Psi(r_{m-1}; r_{n-}, r_{n+}) - 2 \cos k\Delta r \Psi(r_m; r_{n-}, r_{n+}) \right. \right. \\
& \quad \left. \left. + \Psi(r_{m+1}; r_{n-}, r_{n+}) \right] - \langle Z_s(r) p_n(r), w_m \rangle \right\} \\
& = 0, m=2, 3, \dots, M
\end{aligned}
\tag{24}$$

These equations may be assembled into the matrix equation

$$ZI = V$$

where

$$I = \begin{bmatrix} I_1 \\ \vdots \\ I_M \end{bmatrix}, \quad V = \begin{bmatrix} -V_0 \\ 0 \\ 0 \\ \vdots \\ 0 \end{bmatrix}$$

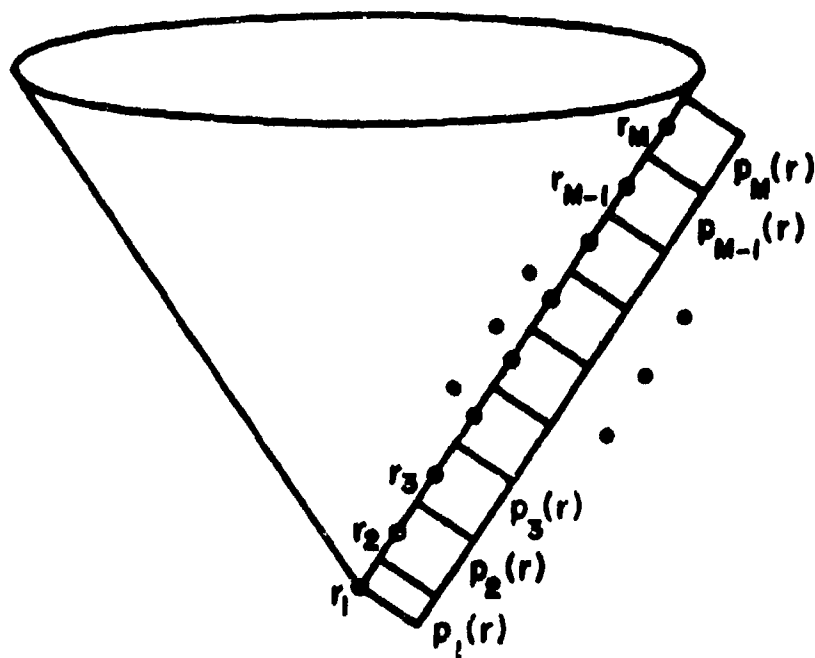


Figure 3. Pulse expansion functions for the current on the cone.

and the elements of the impedance matrix may be identified from (23) and (24). The functions  $\Psi(r; r_{n-}, r_{n+})$  are defined by

$$\Psi(r; r_{n-}, r_{n+}) = \frac{\mu}{8\pi^2} \int_0^{2\pi} \int_{r_{n-}}^{r_{n+}} \frac{r}{r'} \left( \frac{e^{-jkR^+}}{R^+} - \frac{e^{-jkR^-}}{R^-} \right) dr' d\phi' \quad (25)$$

where

$$R^\pm = \sqrt{r^2 + r'^2 - 2rr'(\sin^2\theta_0 \cos\phi' \pm \cos^2\theta_0)} \quad (26)$$

and where

$$r_n^\pm = r_n \pm \Delta r/2$$

The evaluation of the double integral in (24) is simplified by analytically approximating the integration with respect to  $r'$ . This may be accomplished by noting that in general  $k(r_{n+} - r_{n-}) \ll 1$ , so that a few terms of a Taylor series expansion about some point  $r_n$  in the interval  $[r_{n-}, r_{n+}]$  should be accurate. Accordingly, one writes

$$\begin{aligned} e^{-jkR^\pm} &= e^{-jkR_n^\pm} e^{-jk(R^\pm - R_n^\pm)} \\ &\approx e^{-jkR_n^\pm} [1 - jk(R^\pm - R_n^\pm)] \end{aligned} \quad (27)$$

where  $R_n^\pm = R^\pm|_{r=r_n}$ . Substituting (26) into (24) and listing as a fourth argument the point about which the expansion is made, one obtains

$$\begin{aligned}
\Psi(r; r_{n-}, r_{n+}) &\approx \Psi(r; r_{n-}, r_{n+}, r_n) \\
&= \frac{\mu r}{8\pi^2} \int_0^{2\pi} \int_{r_{n-}}^{r_{n+}} \left[ e^{-jkR_n^+} \left( \frac{1+jkR_n^+}{r'R^+} - \frac{jk}{r'} \right) \right. \\
&\quad \left. - e^{-jkR_n^-} \left( \frac{1+jkR_n^-}{r'R^-} - \frac{jk}{r'} \right) \right] dr' d\phi' \\
&= \frac{\mu r}{4\pi^2} \int_0^\pi \left\{ e^{-jkR_n^+} \left[ \frac{1+jkR_n^+}{r} \log \left| \frac{r_{n+}(R_{n-}^+ + r - r_{n-}b^+)}{r_{n-}(R_{n+}^+ + r - r_{n+}b^+)} \right| \right. \right. \\
&\quad \left. \left. - jk \ln \left| \frac{r_{n+}}{r_{n-}} \right| \right] \right. \\
&\quad \left. - e^{-jkR_n^-} \left[ \frac{1+jkR_n^-}{r} \log \left| \frac{r_{n+}(R_{n-}^- + r - r_{n-}b^-)}{r_{n-}(R_{n+}^- + r - r_{n+}b^-)} \right| \right. \right. \\
&\quad \left. \left. - jk \ln \left| \frac{r_{n+}}{r_{n-}} \right| \right] \right\} d\phi' \quad (28)
\end{aligned}$$

where  $b^\pm = \sin^2 \theta_0 \cos \phi' \pm \cos^2 \theta_0$ . In several situations, appropriate limits of the integrand of (27) need to be taken. First, when the source is the current segment at the bicone terminals, the integral (27) reduces to the simple form:

$$\begin{aligned}
\Psi(r; r_1, r_{1+}) &\approx \Psi(r; r_2, r_{1+}, r_1) \\
&= \frac{\mu}{4\pi^2} \int_0^\pi e^{-jkr} (1+jkr) \log \left| \frac{R_{1+}^- + r - b^- r_{1+}}{R_{1+}^+ + r - b^+ r_{2+}} \right| d\phi' \\
&\quad (29)
\end{aligned}$$

As the observation point  $r$  in (28) approaches the bicone terminals,  $r \rightarrow r_1 = 0$ , the limiting form of the integrand can be integrated. The result is

$$\Psi(r_1; r_1, r_{1+}, r_1) = \frac{\mu}{2\pi} \log(\cot \frac{\theta_0}{2}) \quad (30)$$

a very interesting result that is independent of the subdomain size at the bicone terminals. Finally, all the so-called "self terms"  $\Psi(r_n; r_{n-}, r_{n+}, r_n)$ ,  $n \neq 1$ , contain an integrable singularity. In fact one easily establishes that

$$\log \left| \frac{r_{n+}(R_{n-}^+ + r - b^+ r_{n-})}{r_{n-}(R_{n+}^+ + r - b^+ r_{n+})} \right| \xrightarrow{r \rightarrow r_n} -2 \log |\phi'|$$

This singular term is then subtracted from the integrand in (27), resulting in a non-singular integrand which is then numerically integrated. The term

$$\frac{-\mu}{2\pi^2} \int_0^\pi \ln |\phi'| d\phi' = \frac{-\mu}{2\pi} (\ln \pi - 1)$$

is then added to the result to take care of the part of the integral contributed by the singularity.

## SECTION IV

### FORMULATION AND NUMERICAL SOLUTION OF AN INTEGRAL EQUATION FOR A BICONE WITH ENDCAPS

The formulation of the integral equation for a cone radiator over a ground plane with an endcap is considerably more complicated than that for the case when the endcap is not present. It is possible, however, to generalize the approach used for the bicone without a topcap and to transform the derivatives appearing in the equations into harmonic operators along the radial cone and topcap coordinates, as is done in Appendix B. This approach has the advantage again that testing with piecewise sinusoids allows the replacement of derivatives by a finite difference of potentials. However, to effect this transformation, an extremely complicated kernel must be used (see Appendix B) which contains many singularities other than the usual ones where source and field points coincide. While this approach has been used, it has been found to be unwieldy and rather inefficient.

The approach described here begins with the description of fields in terms of the more commonly used vector magnetic and scalar potentials expressed in terms of the cone currents and charge. However, it is found that these potentials are singular at the bicone terminals which again creates an unnecessary complication. In order to circumvent this problem, the cone and image surfaces are allowed to intersect with a



small "waist" of radius "a" (Figure 4). If "a" is very small, there should be negligible difference in the input impedance and currents found for this case and that for the limiting case of  $a=0$ . For convenience, the cone coordinates are defined with respect to the projection of the cone surface to a tip, as in Figure 4. Furthermore, the direction of the unit vector  $\hat{r}_t$  and the positive direction of corresponding vector components is taken to be towards the center of the topcap, in the direction of decreasing  $r_t$ .

The integral equations are obtained by setting the radiated field tangent to the cone surface equal to the impedance drop per unit length due to the loading:

$$-j\omega A_{r_c} - \frac{\partial \phi}{\partial r_c} - Z_s I_c = 0, \quad a/\sin \theta_0 < r_c \leq L + a/\sin \theta_0 \quad (31)$$

$$-j\omega A_{r_t} - \frac{\partial \phi}{\partial r_t} - Z_s I_t = 0, \quad 0 < r_t \leq L \sin \theta_0 + a \quad (32)$$

where the tangential components of magnetic vector potential,  $A_{r_c}$  and  $A_{r_t}$ , are given by

$$A_{r_p} = \frac{\mu}{8\pi^2} \left[ \int_0^{2\pi} \int_{a/\sin \theta_0}^{L+a/\sin \theta_0} I_c \left( \frac{\cos \xi_{pc}^+ e^{-jkR_{pc}^+}}{R_{pc}^+} + \frac{\cos \xi_{pc}^- e^{-jkR_{pc}^-}}{R_{pc}^-} \right) dr'_c d\phi' \right. \\ \left. + \int_0^{2\pi} \int_0^{L\sin \theta_0 + a} I_t \left( \frac{\cos \xi_{pt}^+ e^{-jkR_{pt}^+}}{R_{pt}^+} + \frac{\cos \xi_{pt}^- e^{-jkR_{pt}^-}}{R_{pt}^-} \right) dr'_t d\phi' \right] \\ p = c, t \quad (33)$$

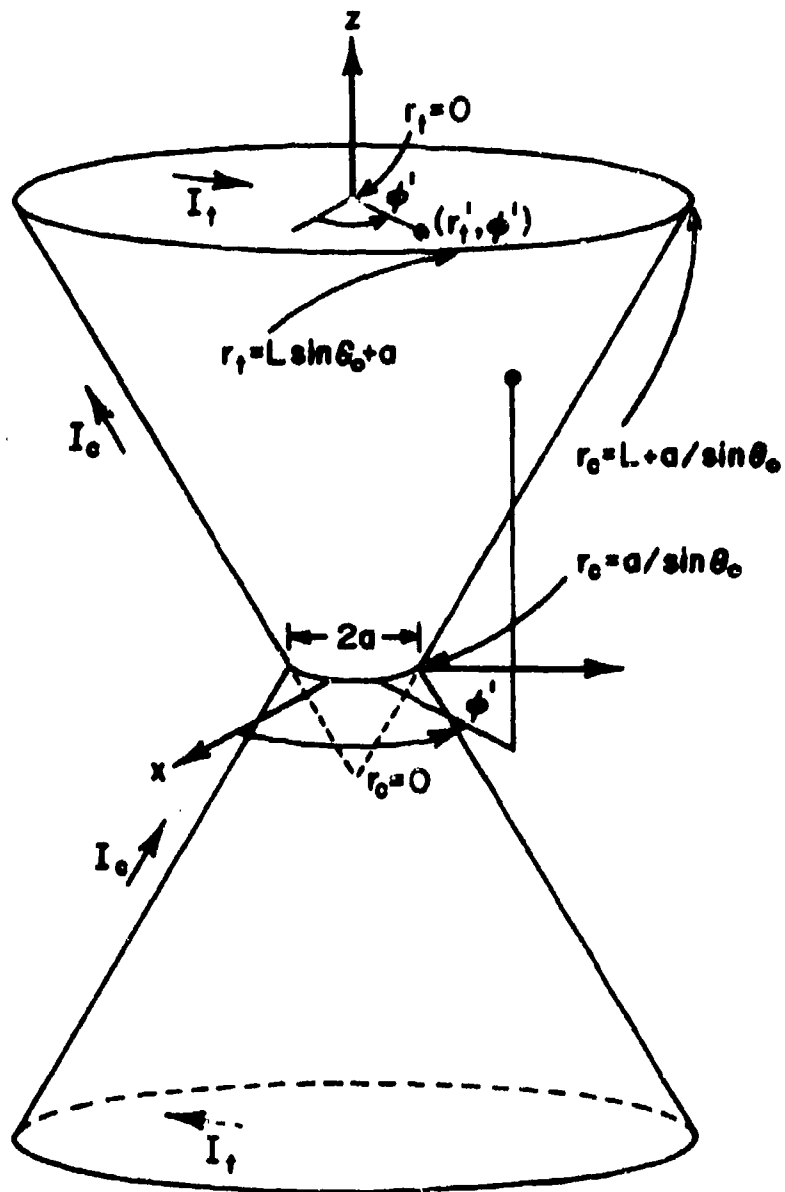


Figure 4. Geometry of cone with endcap.

The scalar potential is given by

$$\phi = \frac{-1}{8\pi^2 j\omega\epsilon} \left[ \int_0^{2\pi} \int_{a/\sin\theta_0}^{L+a/\sin\theta_0} \frac{dI_c}{dr_c} \left( \frac{e^{-jkR_{pc}^+}}{R_{pc}^+} - \frac{e^{-jkR_{pc}^-}}{R_{pc}^-} \right) dr_c' d\phi' \right. \\ \left. + \int_0^{2\pi} \int_0^{k \sin\theta_0 + a} \frac{dI_t}{dr_t} \left( \frac{e^{-jkR_{pt}^+}}{R_{pt}^+} - \frac{e^{-jkR_{pt}^-}}{R_{pt}^-} \right) dr_t' d\phi' \right] \\ p = c, t \quad (34)$$

The currents  $I_c$  and  $I_t$  are the total linear currents on the conical and topcap surfaces, respectively, and are related to the corresponding surface current densities  $J_c$  and  $J_t$  by

$$I_c = 2\pi r_c \sin\theta_0 J_c \\ I_t = 2\pi r_t J_t \quad (35)$$

The distance quantities are all of the form

$$R_{pq}^{\pm} = \sqrt{r_q'^2 + 2b_{pq}^{\pm} r_q' + c_{pq}^{\pm}}, \quad p, q = c, t$$

where

$$b_{cc}^{\pm} = -r_c \sin^2\theta_0 \cos\phi' \mp r_c \cos^2\theta_0 - a \cot\theta_0 \cos\theta_0 (1 \mp 1)$$

$$c_{cc}^{\pm} = r_c^2 + a^2 \cot^2 \theta_0 (1 \mp 1)^2 - 2r_c a \cos \theta_0 \cot \theta_0 (1 \mp 1)$$

$$b_{ct}^{\pm} = -r_c \sin \theta_0 \cos \phi'$$

$$c_{ct}^{\pm} = r_c^2 - 2r_c \cos \theta_0 (a \cot \theta_0 \pm L \cos \theta_0) + (a \cot \theta_0 \pm L \cos \theta_0)^2$$

$$b_{tc}^{\pm} = \mp L \cos^2 \theta_0 - a \cos \theta_0 \cot \theta_0 - r_t \sin \theta_0 \cos \phi'$$

$$c_{tc}^{\pm} = r_t^2 + (L \cos \theta_0 \pm a \cot \theta_0)^2$$

$$b_{tt}^{\pm} = -r_t \cos \phi'$$

$$c_{tt}^{\pm} = r_t^2 + L^2 \cos^2 \theta_0 (1 \mp 1)^2$$

The angles between the source current elements and the tangential component of electric field at the observation point are determined by

$$\cos \xi_{cc}^{\pm} = \pm \cos \phi' \sin^2 \theta_0 + \cos^2 \theta_0$$

$$\cos \xi_{ct}^{\pm} = \mp \sin \theta_0 \cos \phi'$$

$$\cos \xi_{tt}^{\pm} = \pm \cos \phi'$$

$$\cos \xi_{tc}^{\pm} = \mp \cos \phi' \sin \theta_0$$

It is convenient to choose as testing functions the pulse functions  $p_n$  shown in Figure 5. Thus, testing (31) with  $p_1$  results in

$$-j\omega \langle A_{r_c}, p_1 \rangle - \left\langle \frac{\partial \phi}{\partial r_c}, p_1 \right\rangle - \langle Z_s I_c, p_1 \rangle = 0$$

Upon integrating by parts in the central term, and noting that  $A_{r_c}$  is slowly varying over the interval and hence may be approximated by  $A_{r_c}(r_{c1})$ , one obtains

$$-j\omega A_{r_c}(r_{c1}) \frac{\Delta r_c}{2} - [(\phi(r_{c1} + \Delta r_c/2) - \phi(r_{c1}))] - \langle Z_s I_c, p_1 \rangle = 0$$

But  $\phi(r_{c1})$  is just the bicone terminal voltage  $V_0$  with respect to the ground plane. Hence,

$$-j\omega A_{r_c}(r_{c1}) \Delta r_c - 2\phi(r_{c1} + \Delta r_c/2) - \langle Z_s I_c, p_1 \rangle = -2V_0 \quad (36)$$

For the remaining testing functions on the cone, testing of (31), integration by parts on the scalar potential term and approximation of the vector potential by its value at the center of the pulse yields

$$\begin{aligned} -j\omega \Delta r_c A_{r_c}(r_{cm}) - [\phi(r_{cm} + \Delta r_c/2) - \phi(r_{cm} - \Delta r_c/2)] \\ - \langle Z_s I_c, p_m \rangle = 0, \quad m = 2, 3, \dots, N_c - 1 \end{aligned} \quad (37)$$

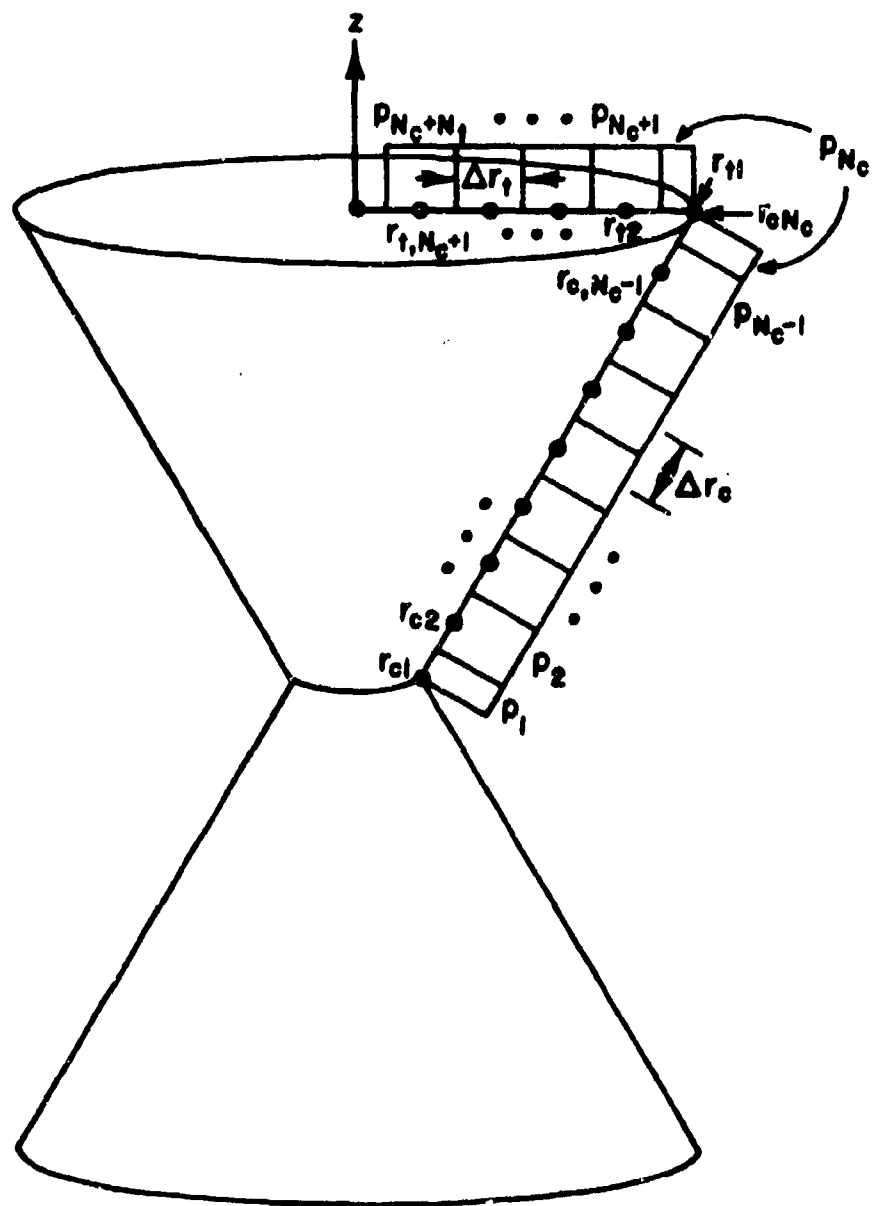


Figure 5. Pulse expansion and testing functions.

At the edge, the testing pulse consists of two parts, one on the cone surface and one on the topcap. Hence, both equations (31) and (32) must be used. With approximations on the two vector potential components similar to that above, integration by parts, and enforcement of continuity of the scalar potential at the edge, one obtains

$$-j\omega \left[ \frac{\Delta r_c}{2} A_{r_c}(r_{cN_c}) + \frac{\Delta r_t}{2} A_{r_t}(r_{t1}) \right] - [\Phi(r_{cN_c} - \Delta r_c/2) - \Phi(r_{t1} + \Delta r_t/2)] - \langle Z_s I_r, P_{N_c} \rangle = 0 \quad (38)$$

where  $I_r = I_c$  or  $I_t$  as is appropriate. On the topcap, one has, analogous to (37),

$$-j\omega \Delta r_t A_{r_t}(r_{tm}) - [\Phi(r_{tm} - \Delta r_t/2) - \Phi(r_{tm} + \Delta r_t/2)] - \langle Z_s I_t, P_{N_c-1+m} \rangle = 0, \quad m=2, \dots, N_c+1 \quad (39)$$

The current is next expanded in the set of pulse functions  $p_n$  of Figure 5,

$$I_c(r_c) \approx \sum_{n=1}^{N_c} I_n p_n(r_c) \quad (40)$$

$$I_t(r_t) = \sum_{n=N_c}^{N_c+N_t} I_n p_n(r_t) \quad (41)$$

Note that the current  $I_{N_c}$  at the edge of the cone is the same on both the cone and the topcap surfaces. The derivatives of the currents above are approximated by a finite difference of adjacent current pulses which is then assumed to be expanded in its own set of "charge" pulses (see Figure 6);

$$\frac{dI_c}{dr_c} \approx \sum_{n=1}^{N_c-1} \left( \frac{I_{n+1} - I_n}{\Delta r_c} \right) p_n^+(r_c) \quad (42)$$

$$\frac{dI_t}{dr_t} \approx \sum_{n=N_c}^{N_c+N_t} \left( \frac{I_{n+1} - I_n}{\Delta r_t} \right) p_n^+(r_t) \quad (43)$$

where  $I_{N_c+N_t+1}$  is taken to be zero.

Thus the vector potential quantities in (36)-(39) may be written as

$$\begin{aligned} A_{r_t} = \frac{\mu}{8\pi^2} & \left\{ I_1 \psi_{pc}(r_p, r_{c1}, r_{c1} + \Delta r_c/2) \right. \\ & + \sum_{n=2}^{N_c-1} I_n \psi_{pc}(r_p, r_{cn} - \Delta r_c/2, r_{cn} + \Delta r_c/2) \\ & + I_{N_c} [\psi_{pc}(r_p, r_{cN_c} - \Delta r_c/2, r_{cN_c}) + \psi_{pt}(r_p, r_{t1}, r_{t1} + \Delta r_t/2)] \\ & \left. + \sum_{n=N_c+1}^{N_c+N_t} I_n \psi_{pt}(r_p, r_{t,n+1-N_c} - \Delta r_t/2, r_{t,n+1-N_c} + \Delta r_t/2) \right\} \\ & p = c, t \quad (44) \end{aligned}$$



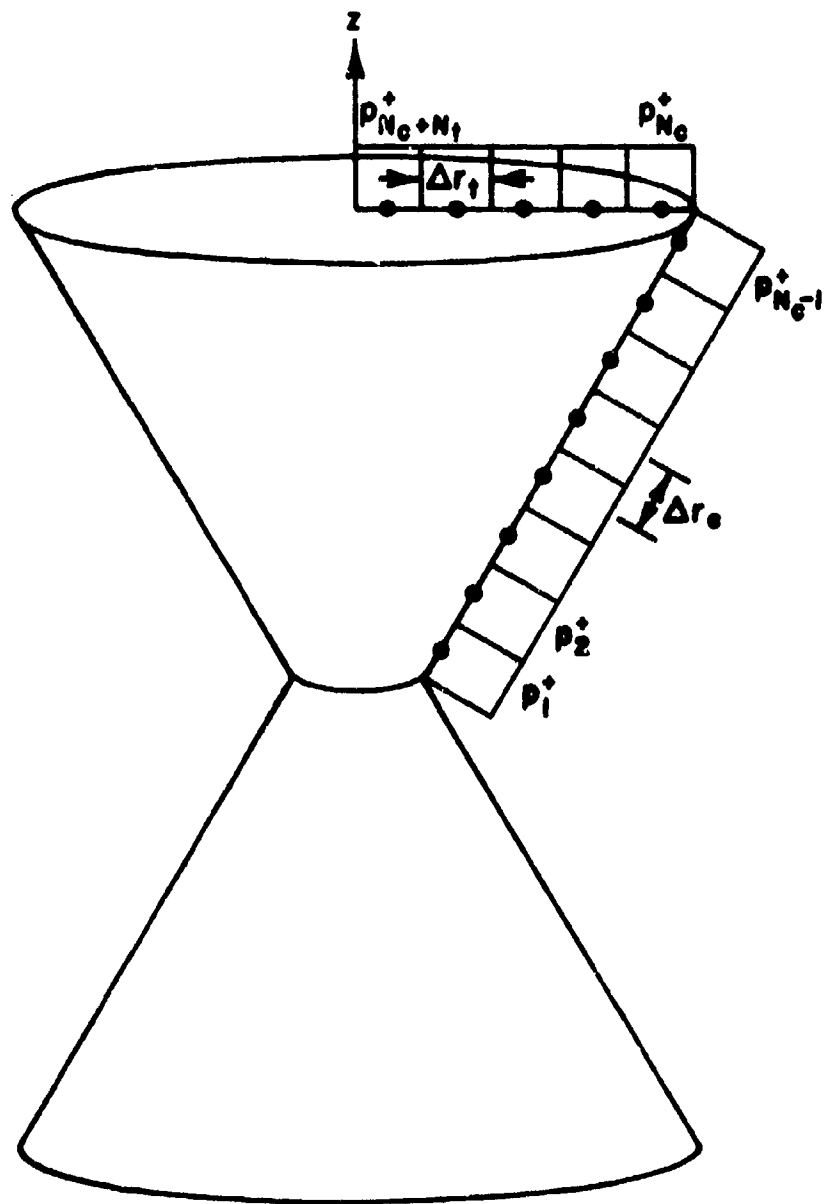


Figure 6. Pulse expansions for the charge on the cone.

and the scalar potential is

$$\Phi = \frac{-1}{8\pi^2 j\omega\epsilon} \left[ \sum_{n=1}^{N_c-1} \left( \frac{I_{n+1} - I_n}{\Delta r_c} \right) \psi_{pc}(r_p, r_{cn}, r_{cn} + \Delta r_c) \right. \\ \left. + \sum_{n=N_c}^{N_c+N_t} \left( \frac{I_{n+1} - I_n}{\Delta r_t} \right) \psi_{pt}(r_p, r_{t,n+1-N_c}, r_{t,n+1-N_c} + \Delta r_c) \right] \\ p = c, t \quad (45)$$

where

$$\psi_{pq}(r_p, r_{n-}, r_{n+}) = \int_0^{2\pi} \left( \cos \xi_{pq}^+ \int_{r_{n-}}^{r_{n+}} \frac{e^{-jkR_{pq}^+}}{R_{pq}^+} dr' \right. \\ \left. + \cos \xi_{pq}^- \int_{r_{n-}}^{r_{n+}} \frac{e^{-jkR_{pq}^-}}{R_{pq}^-} dr' \right) d\phi' \\ p, q = c, t \quad (46)$$

and

$$\psi_{pq}(r_p, r_{n-}, r_{n+}) = \int_0^{2\pi} \int_{r_{n-}}^{r_{n+}} \left[ \frac{e^{-jkR_{pq}^+}}{R_{pq}^+} \right. \\ \left. - \frac{e^{-jkR_{pq}^-}}{R_{pq}^-} \right] dr' d\phi' \\ p, q = c, t \quad (47)$$

The inner integrals in (46) and (47) can be approximately analytically integrated. They are all of the form

$$\int_{r_{n-}}^{r_{n+}} \frac{e^{-jkR}}{R} dr' \quad (48)$$

where  $R$  is of the form

$$R = \sqrt{r'^2 + 2r'b + c} \quad (49)$$

Since the range of integration  $[r_{n-}, r_{n+}]$  is small compared to a wavelength, it is appropriate to expand  $e^{-jkR}$  in a Taylor series about some point  $R_n$  which is the distance from the observation point to a point  $r_n$  in the interval  $[r_{n-}, r_{n+}]$ . Thus,

$$\begin{aligned} e^{-jkR} &= e^{-jk(R-R_n)} e^{-jkR_n} \\ &= e^{-jkR_n} [\cos k(R-R_n) - j \sin k(R-R_n)] \\ &\approx e^{-jkR_n} \left[ 1 - \frac{k^2(R-R_n)^2}{2} - jk(R-R_n) \right. \\ &\quad \left. + jk^3(R-R_n)^3/6 \right] \end{aligned}$$

The error in the real and imaginary parts is less than

$$\max_{r' \in [r_{n-}, r_{n+}]} \frac{k^4(R-R_n)^4}{24} \leq \frac{k^4(\Delta r/2)^4}{24}$$

where  $\Delta r$  is the subdomain size. For five subdomains per wavelength ( $\Delta r/\lambda = 1/5$ ), this results in a maximum error of less than 1% in both the real and imaginary parts of the integrand. The resulting integral should indeed be much more accurate than this. With this approximation,

$$\int_{r_{n-}}^{r_{n+}} \frac{e^{-jkR}}{R} dr' \approx e^{-jkR_n} (I_1 - jI_2)$$

where

$$\begin{aligned} I_1 &= \int_{r_{n-}}^{r_{n+}} \frac{1 - k^2(R - R_n)^2/2}{R} dr' \\ &= \left( 1 - \frac{k^2 R_n^2}{2} \right) \ln \left| \frac{R_{n+} + r_{n+} + b}{R_{n-} + r_{n-} + b} \right| + k^2 R_n (r_{n+} - r_{n-}) \\ &\quad - k^2 \left[ \frac{r_{n+} + b}{2} R_{n+} - \frac{r_{n-} + b}{2} R_{n-} + \frac{c-b^2}{2} \ln \left| \frac{R_{n+} + r_{n+} + b}{R_{n-} + r_{n-} + b} \right| \right] \end{aligned}$$

and where

$$\begin{aligned} I_2 &= \int_{r_{n-}}^{r_{n+}} \frac{k(R - R_n) - k^3(R - R_n)^3/6}{R} dr' \\ &= (-k R_n + k^3 R_n^3/6) \ln \left| \frac{R_{n+} + r_{n+} + b}{R_{n-} + r_{n-} + b} \right| + (k - k^3 R_n^2/2) (r_{n+} - r_{n-}) \end{aligned}$$

$$+ \frac{k^3 R_n}{2} \left[ \frac{r_{n+} + b}{2} R_{n+} - \frac{r_{n-} + b}{2} R_{n-} + \frac{(c-b)^2}{2} \ell_n \left| \frac{R_{n+} + r_{n+} + b}{R_{n-} + r_{n-} + b} \right| \right]$$

$$- \frac{k^3}{6} \left[ \frac{r_{n+}^3 - r_{n-}^3}{3} - b(r_{n+}^2 - r_{n-}^2) + c(r_{n+} - r_{n-}) \right]$$

Combining these results, one has, finally,

$$\int_{r_{n-}}^{r_{n+}} \frac{e^{-jkR}}{R} dr' \approx$$

$$\begin{aligned} e^{-jkR_n} \left\{ \left[ 1 + jkR_n - \frac{k^2 R_n^2}{2} - j \frac{k^3 R_n^3}{6} \right. \right. \\ \left. - \left( \frac{k^2}{2} + j \frac{k^3 R_n}{2} \right) \left( \frac{c-b}{2} \right) \right] \ell_n \left| \frac{R_{n+} + r_{n+} + b}{R_{n-} + r_{n-} + b} \right| \\ - \frac{1}{4} (k^2 + jk^3 R_n) [(r_{n+} + b)R_{n+} - (r_{n-} + b)R_{n-}] \\ + \frac{jk^3}{6} \left[ \frac{r_{n+}^3 - r_{n-}^3}{3} + b(r_{n+}^2 - r_{n-}^2) \right] \\ \left. + \left( -jk + k^2 R_n + j \frac{k^3 R_n^2}{2} + j \frac{k^3 c}{6} \right) (r_{n+} - r_{n-}) \right\} \quad (50) \end{aligned}$$

Equation (50) is singular in  $\phi'$  if the observation point is in the interval  $[r_{n-}, r_{n+}]$ . Hence, the integrals in (46) and

(47) need to be evaluated by subtracting the singularity from the integrand and adding its integral to the numerically determined integral. If  $r_n$  is in the interior of the interval,  $r_{n-} < r_n < r_{n+}$ , (50) behaves like  $-2\ln|\phi'|$  near  $\phi' = 0$ ; if  $r_n = r_{n-}$  or  $r_n = r_{n+}$ , (50) behaves like  $-\ln|\phi'|$ . The details of the procedure parallels that described at the end of Section III.

## SECTION V

### NUMERICAL RESULTS AND CONCLUSIONS

This section describes numerical results obtained from the computer code developed from the theory described in Section IV. The resulting code was written to model the cone with or without a topcap. Hence, results from this general code could be checked against those obtained from the code based on the methods of Section III for the cone without a topcap. For narrow cone angles, the calculated input impedance for unloaded cones for various frequencies was also compared to the theory of Schelkunoff [5] and found to be in very good agreement. Results from the general code for moderate cone angles were also compared with those computed by the method of Appendix B, which includes the effects of the topcap. These comparisons were made to validate the consistency of the various approaches and to compare with existing data. It was also established that the input reactance at low frequencies could be used to check the static capacitance calculated in the companion report [1] for both the loaded and unloaded case. Finally, it was verified that the computed results were almost independent of the choice of the waist radius,  $a$ , of Section III, provided  $a$  was chosen small enough.

All the data in this section pertain to a conical antenna with a vertical height of 40 meters and a cone angle of  $\theta_0 = 42.26^\circ$ . These parameters translate to a cone slant height of 54.05 meters and correspond approximately to the cone considered in [6]. The locations and values of the lumped resistive loads used are listed in Table 1 and are taken from [6].

Figures 7-10 illustrate the current distribution on the cone at a frequency of 825 KHz, approximately the first resonant frequency of the unloaded structure. Figures 11-14 illustrate the same results at 1.375 MHz, approximately half-way between first and second resonance of the unloaded structure (see Figures 15 and 16). Two features of the current distributions are notable. First, the edge condition [7], which requires that the current at the edge has infinite slope, and the continuity equation relating current and charge, which requires that the total current approach zero with zero slope at the center of the topcap, combine to limit the amount of current the topcap can support. Secondly, the loading, which increases to a maximum at the edge, further limits current flow on the topcap.

Figures 15-18 illustrate the variation with frequency of the input impedance of the conical structure for the various loading and topcap configurations. Again, the influence of the topcap is found to be negligible. The absence of



Table 1. Positions and values of loading resistors on the cone.

ARC LENGTH ALONG THE CONE GENERATOR (METERS)	RESISTANCE (OHMS)
12.17	4.69
14.34	7.17
16.90	9.06
19.93	11.74
23.54	15.43
27.73	20.82
32.59	30.36
38.41	50.38
45.31	114.88
53.43	114.88
63.15	100.00
72.25	100.00
81.35	100.00

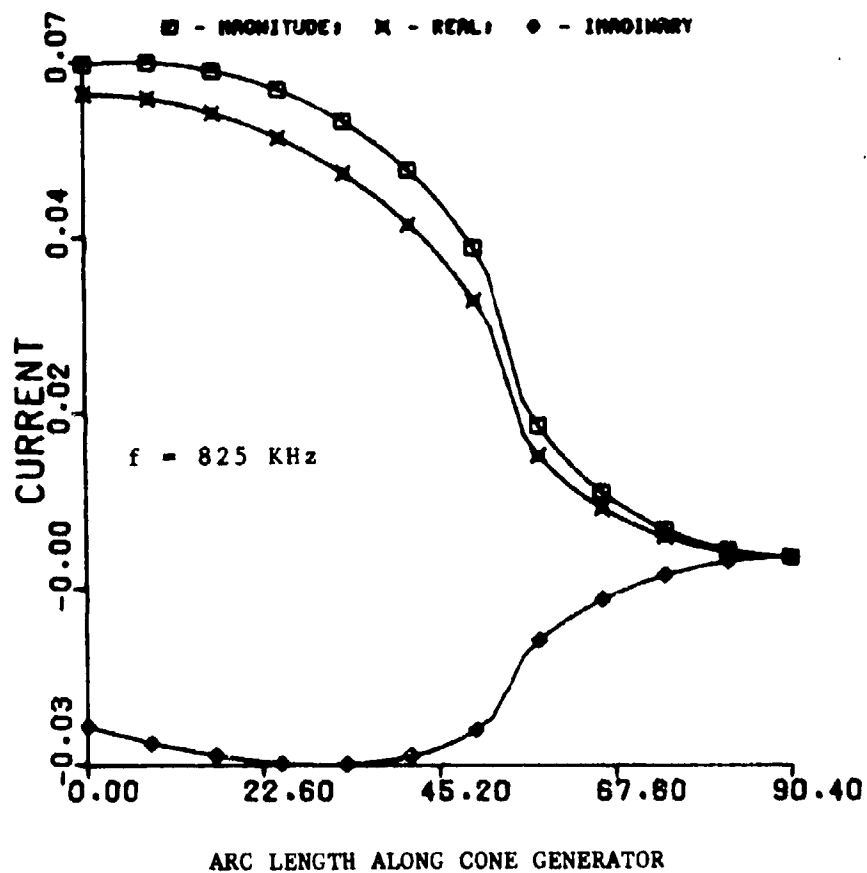


Figure 7. Current on unloaded cone with topcap,  $L=54.05\text{m}$ ,  $\theta_0 = 42.26^\circ$ ,  $V_0 = 1 \text{ Volt}$ ,  $f = 825 \text{ KHz}$ .

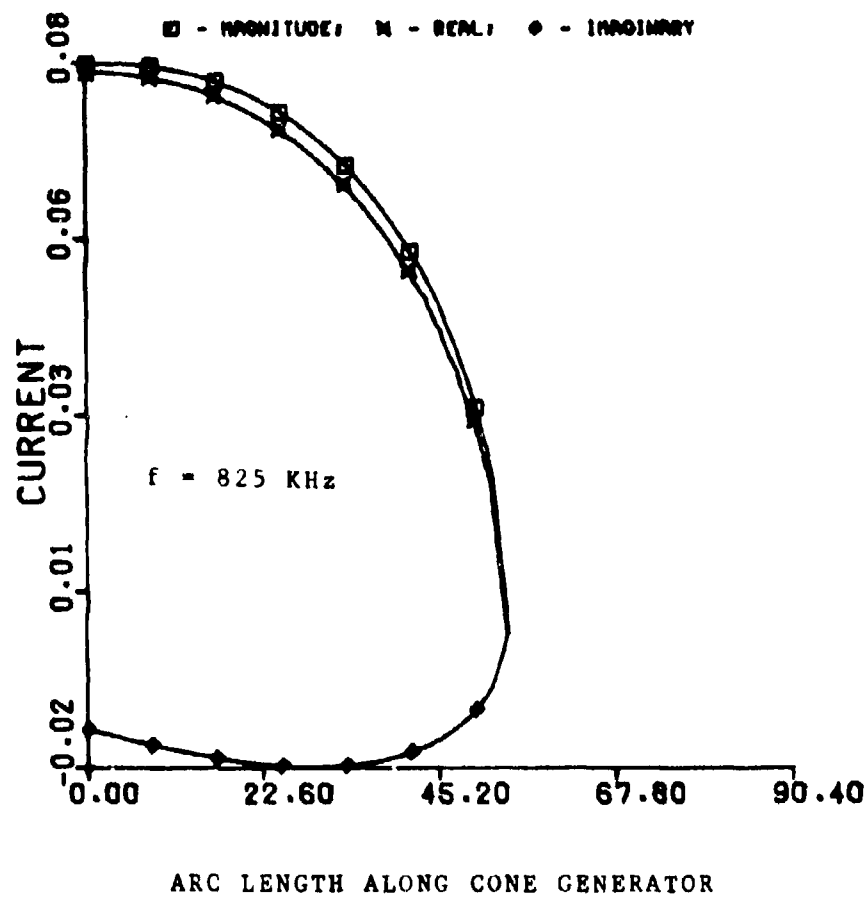


Figure 8. Current on unloaded cone without topcap,  
 $L=54.05\text{m}$ ,  $\theta_0 = 42.26^\circ$ ,  $V_0 = 1 \text{ Volt}$ ,  $f = 825 \text{ KHz}$ .

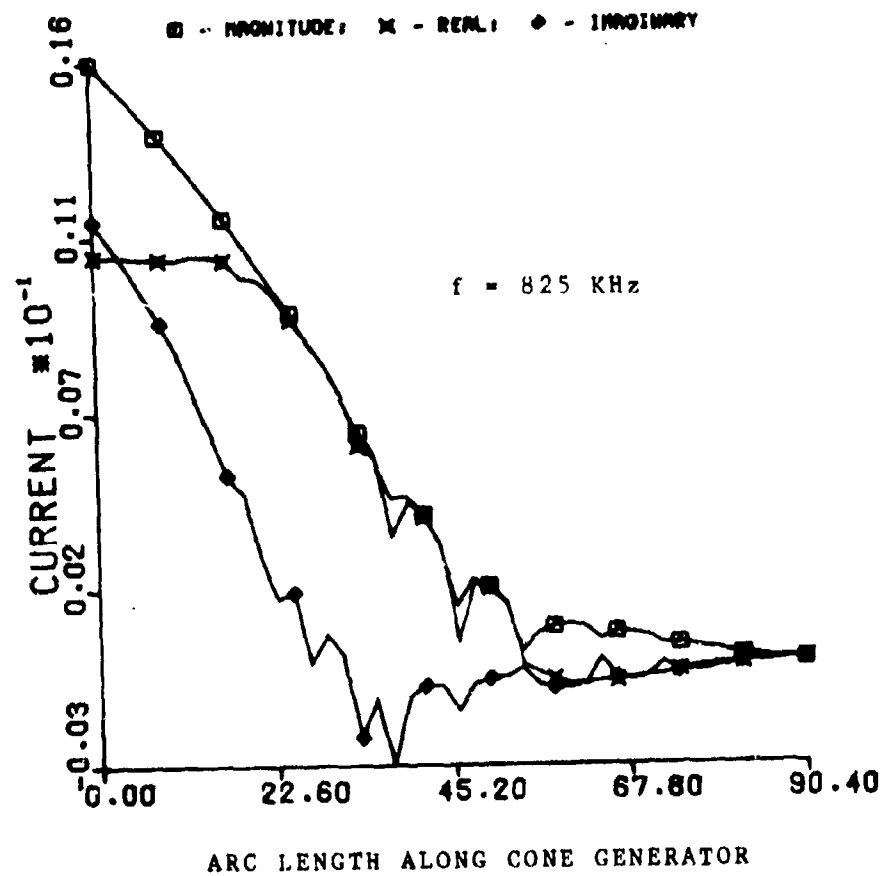


Figure 9. Current on loaded cone with topcap,  $L=54.05\text{m}$ ,  
 $\theta_0 = 42.26^\circ$ ,  $V_0 = 1 \text{ Volt}$ ,  $f = 825 \text{ KHz}$ .

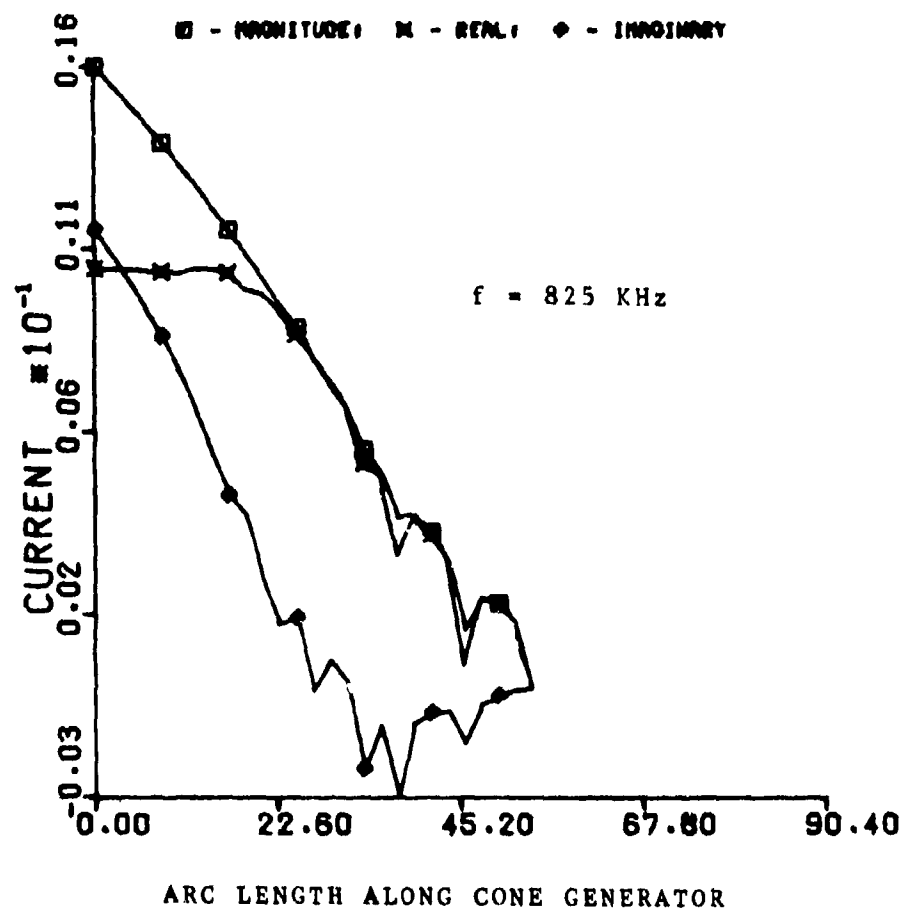


Figure 10. Current on loaded cone without topcap,  
 $L=54.05\text{m}$ ,  $\theta_0 = 42.26^\circ$ ,  $V_0 = 1 \text{ Volt}$ ,  
 $f = 825 \text{ MHz}$ .

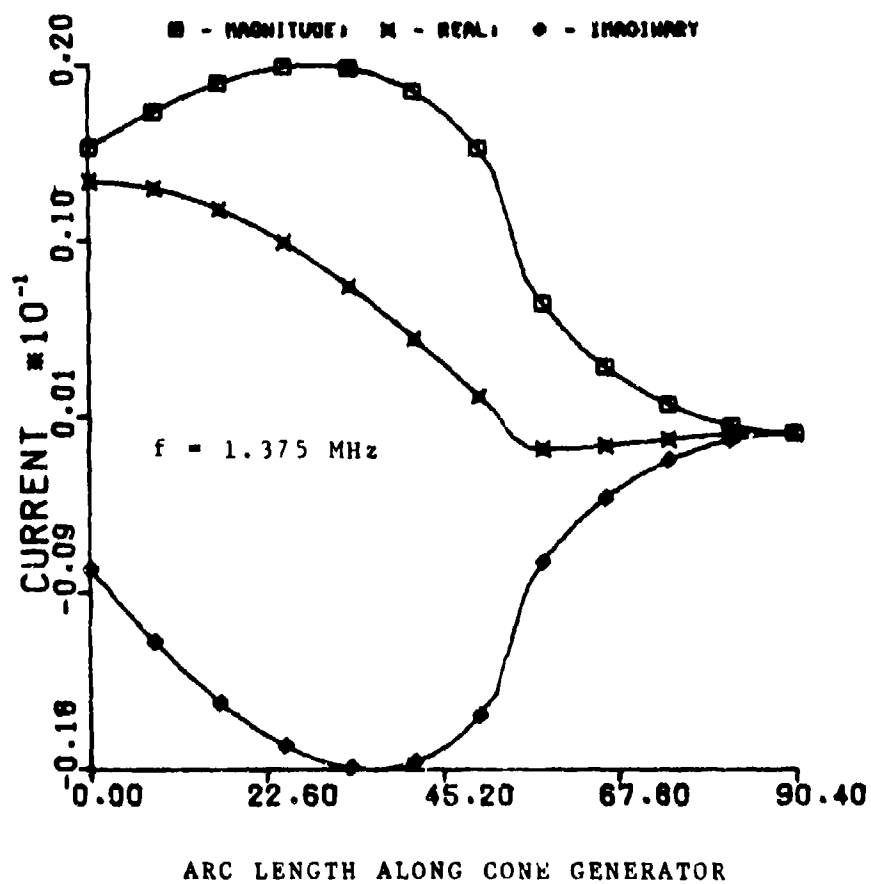


Figure 11. Current on unloaded cone with topcap,  $L=54.05\text{m}$ ,  $\theta_0 = 42.26^\circ$ ,  $V_0 = 1 \text{ Volt}$ ,  $f = 1.375 \text{ MHz}$ .

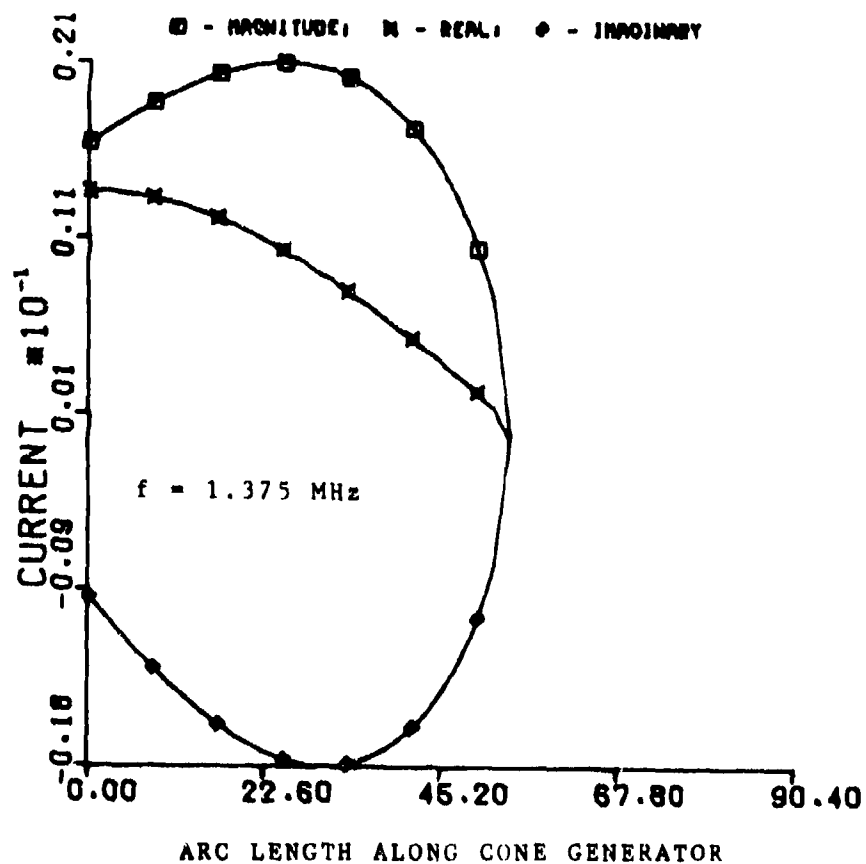


Figure 12. Current on unloaded cone without topcap,  
 $L=54.05\text{m}$ ,  $\theta_0 = 42.26^\circ$ ,  $V_0 = 1 \text{ Volt}$ ,  
 $f = 1.375 \text{ MHz}$ .

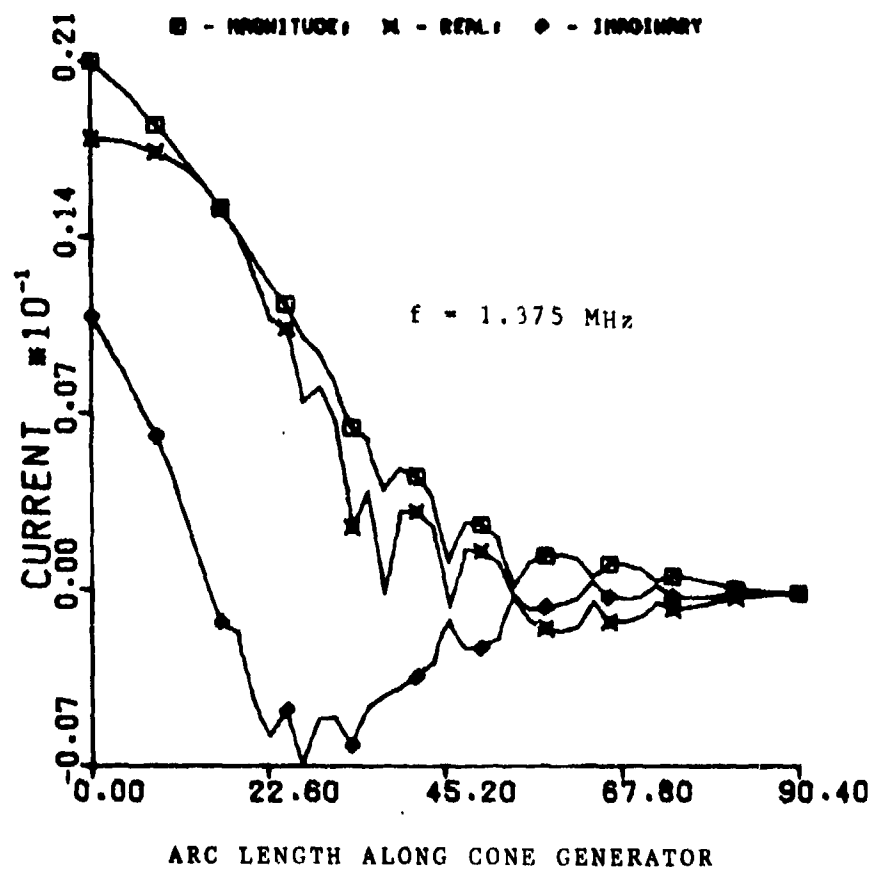


Figure 13. Current on loaded cone with topcap,  $L=54.05\text{m}$ ,  
 $\theta_0 = 42.26^\circ$ ,  $V_0 = 1 \text{ Volt}$ ,  $f = 1.375 \text{ MHz}$ .



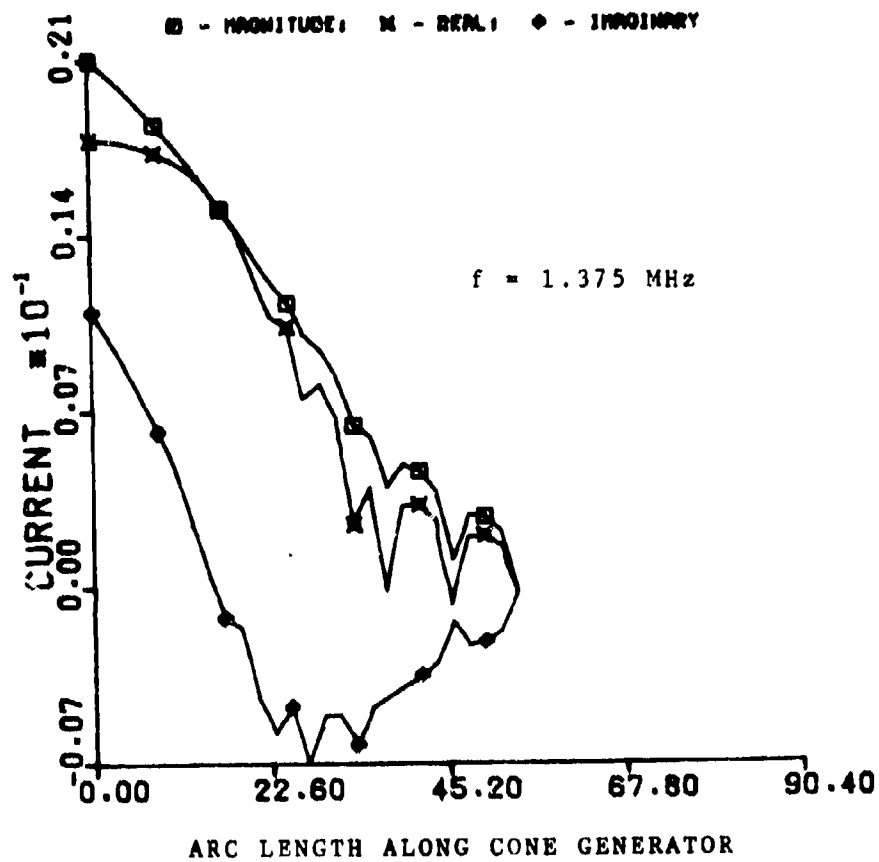


Figure 14. Current on loaded cone without topcap,  
 $L=54.05\text{m}$ ,  $\theta_0 = 42.26^\circ$ ,  $V_0 = 1 \text{ Volt}$ ,  
 $f = 1.375 \text{ MHz}$ .

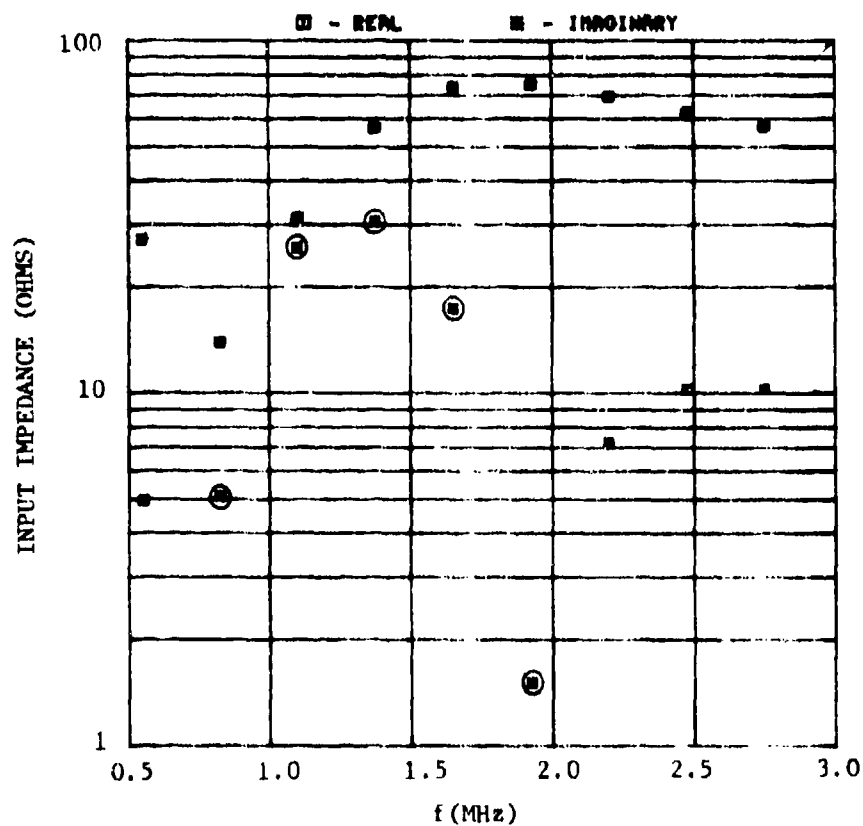


Figure 15. Input impedance of unloaded cone with topcap,  $L=54.05\text{m}$ ,  $\theta_0 = 42.26^\circ$ . Encircled values of imaginary part are positive.

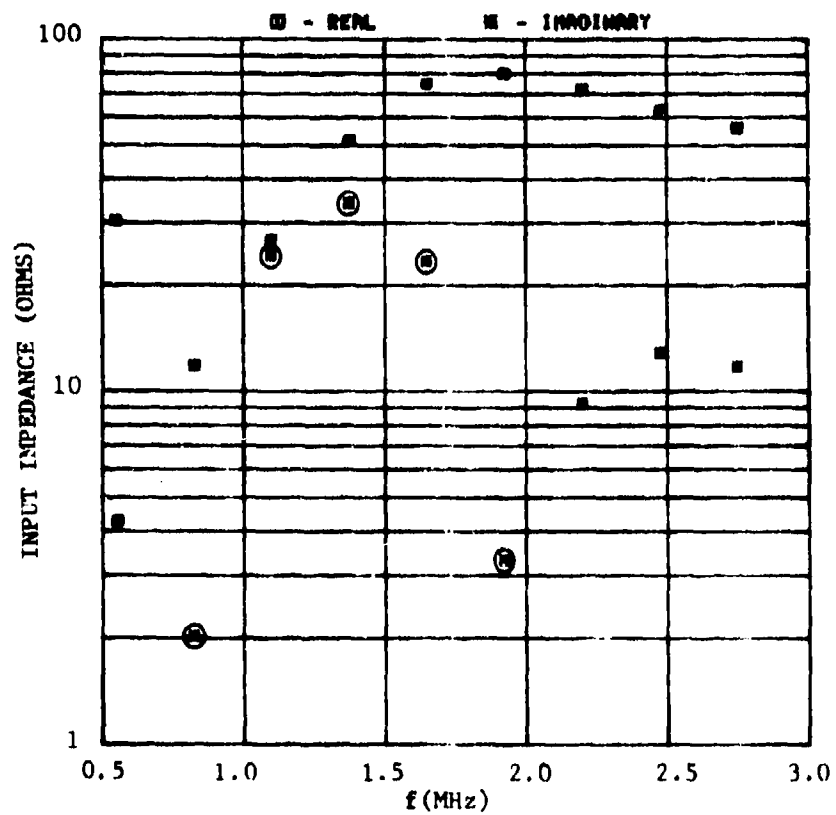


Figure 16. Input impedance of unloaded cone without topcap,  $L=54.05m$ ,  $\theta_0 = 42.26^\circ$ . Encircled values of imaginary part are positive.

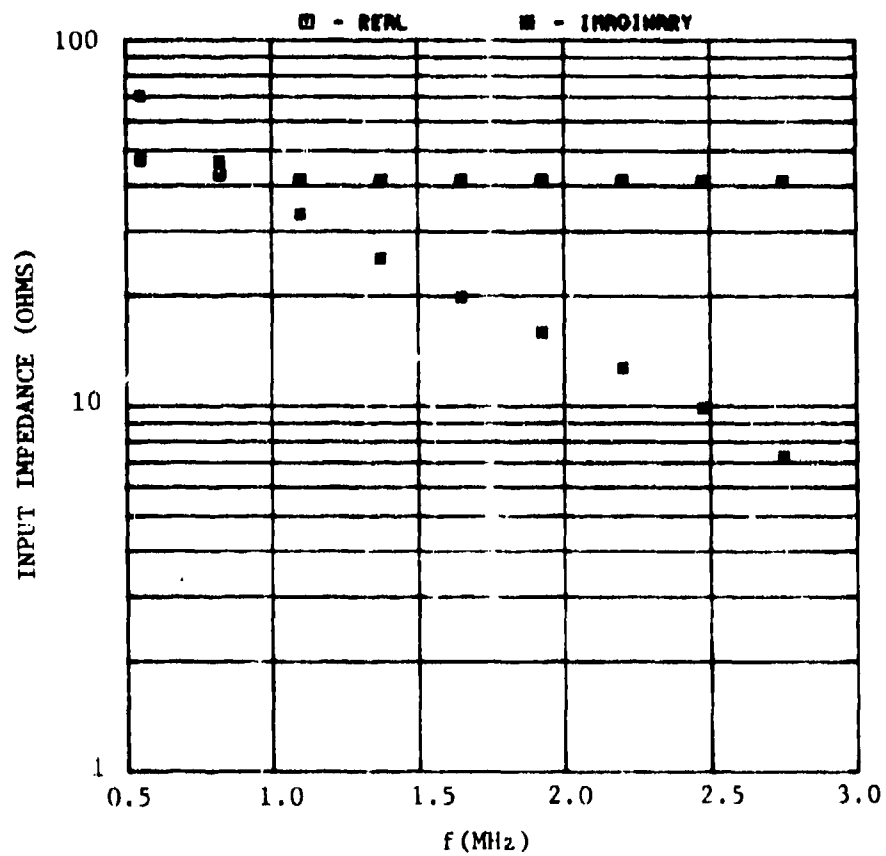


Figure 17. Input impedance of loaded cone with topcap,  $L=54.05n$ ,  $\theta_0 = 42.26^\circ$ . Imaginary values are negative.

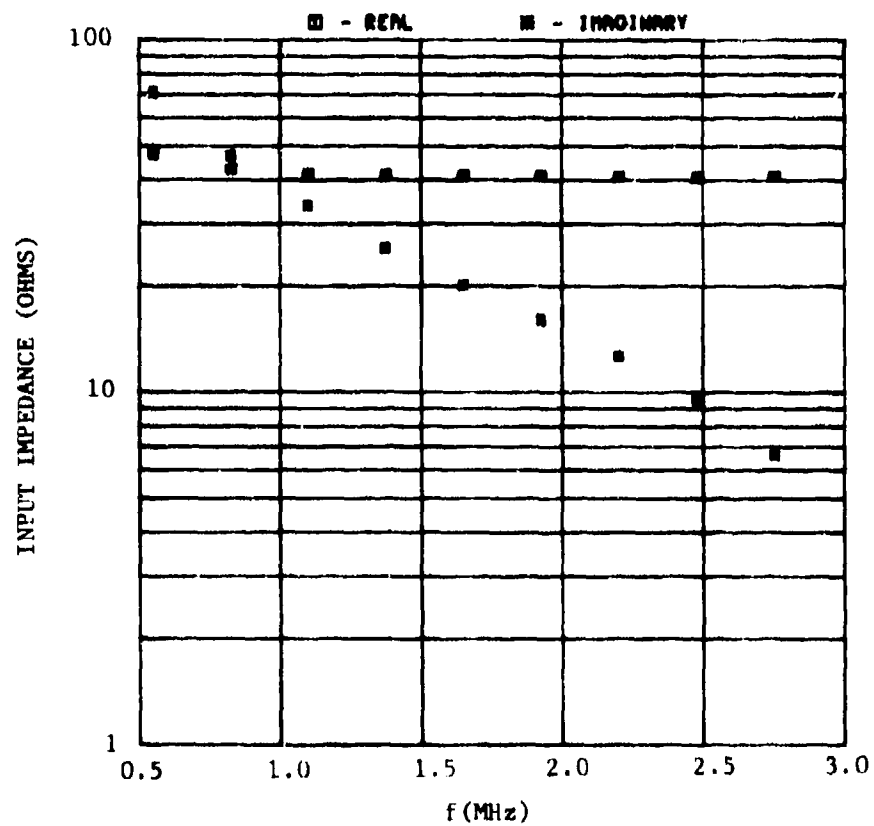


Figure 18. Input impedance of loaded cone without topcap,  $L=54.05m$ ,  $\theta_0=42.26^\circ$ . Imaginary values are negative.

resonances in the loaded case can be attributed to the effectiveness of the resistive loading in eliminating reflections from the cone edge which would result in standing waves on the structure.

Radiation patterns in the near-field region of the loaded structure with a topcap ( $r = 100$  meters and the frequency is 550 KHz) are shown in Figures 19-21. Figures 22-24 give the corresponding patterns in the far field ( $r = 10^4$  meters). For comparison, far field patterns for the unloaded structure are illustrated in Figures 25-27.

Although resources did not permit a time-domain analysis of the response of the structure, such a study, which could include a simple equivalent circuit model of the pulser, would be a logical extension of the present problem. To be done efficiently, however, some improvements in the present computer code should be implemented. Specifically, an adaptive integration procedure should be employed to handle the integrations over the conical current subdomains, whose radii vary drastically from regions near the feed to those near the cone edge. The present code uses a fixed order quadrature rule for all segments on the structure. Additional parameter studies can be carried out using the present code to assess the effects of lumped vs. distributed loading and the effects of various load distributions on the performance of the simulator. A more

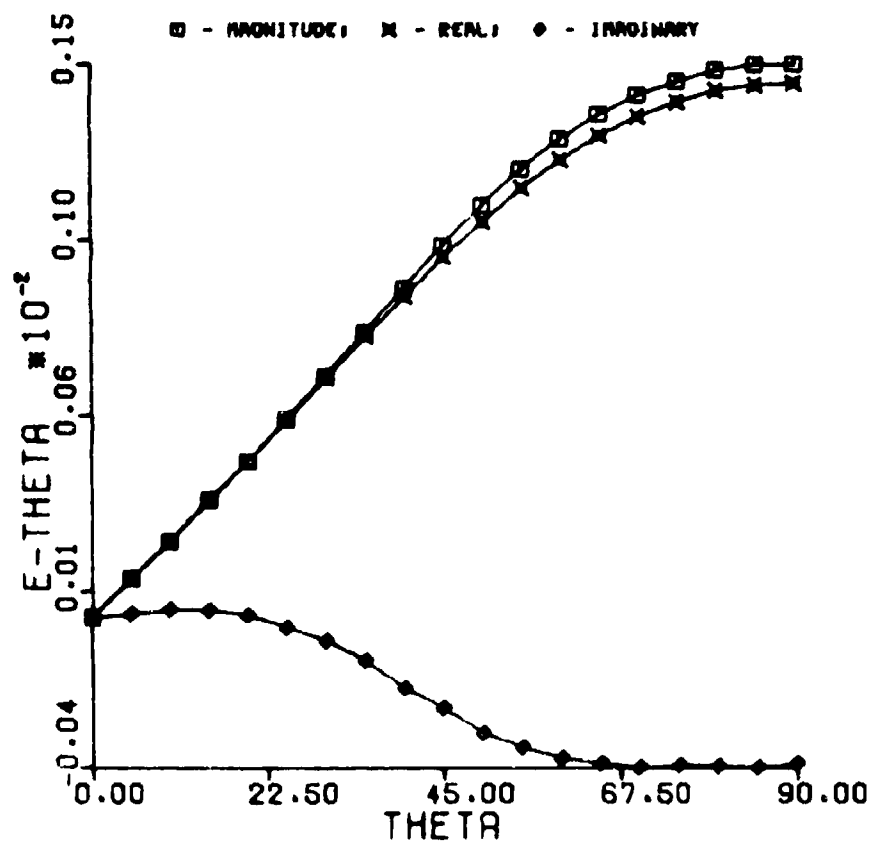


Figure 19.  $E_{\theta}$  radiation pattern for loaded cone with topcap,  $L=54.05m$ ,  $\theta_0 = 42.26^\circ$ ,  $V_0=1$  Volt,  $f = 550$  KHz,  $r = 100m$ .

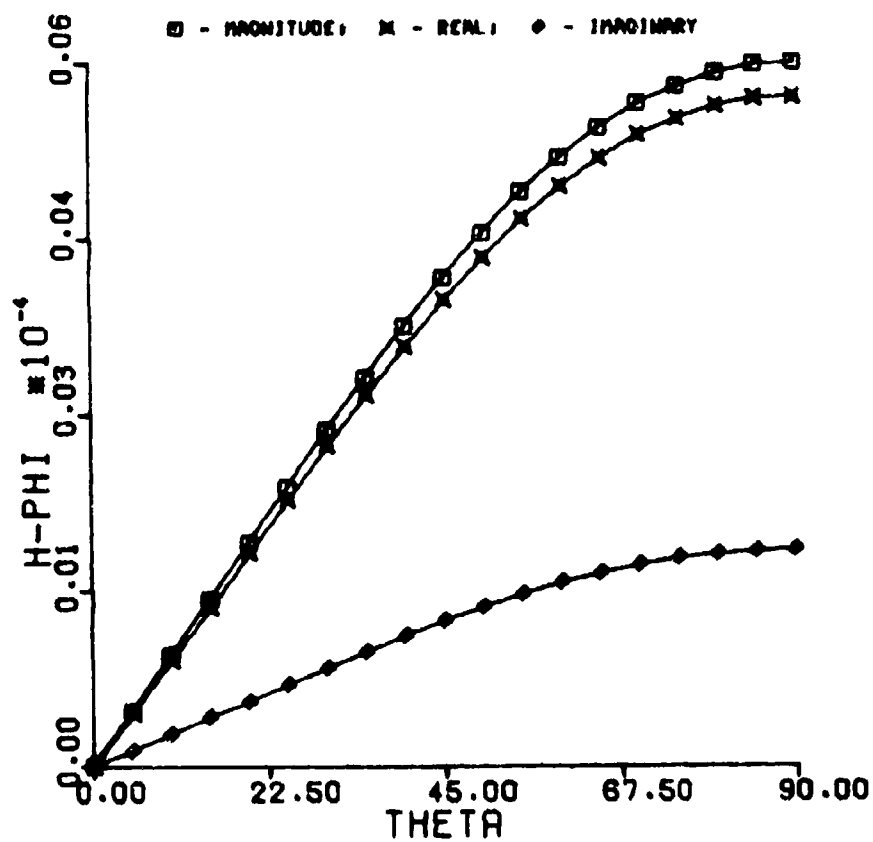


Figure 20.  $H_{\phi}$  radiation pattern for loaded cone with topcap,  $L=54.05m$ ,  $\theta_0 = 42.26^\circ$ ,  $V_0 = 1$  Volt,  $f = 550$  KHz,  $r = 100m$ .



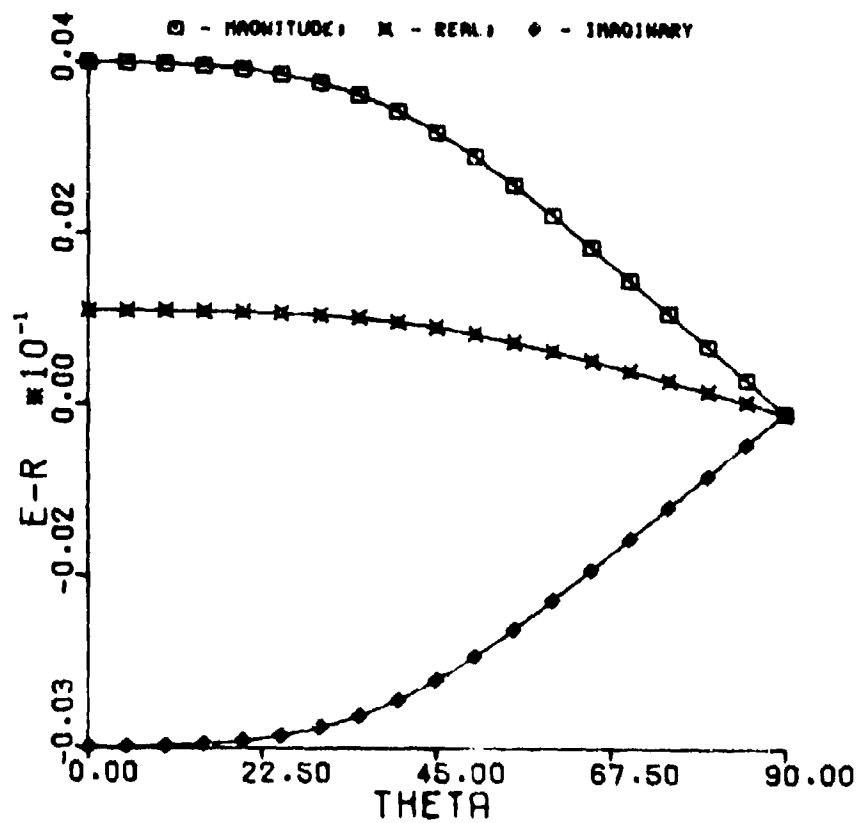


Figure 21.  $E_r$  radiation pattern for loaded cone with topcap,  $L=54.05m$ ,  $\theta_0 = 42.26^\circ$ ,  $V_0 = 1$  Volt,  $f = 550$  KHz,  $r = 100m$ .

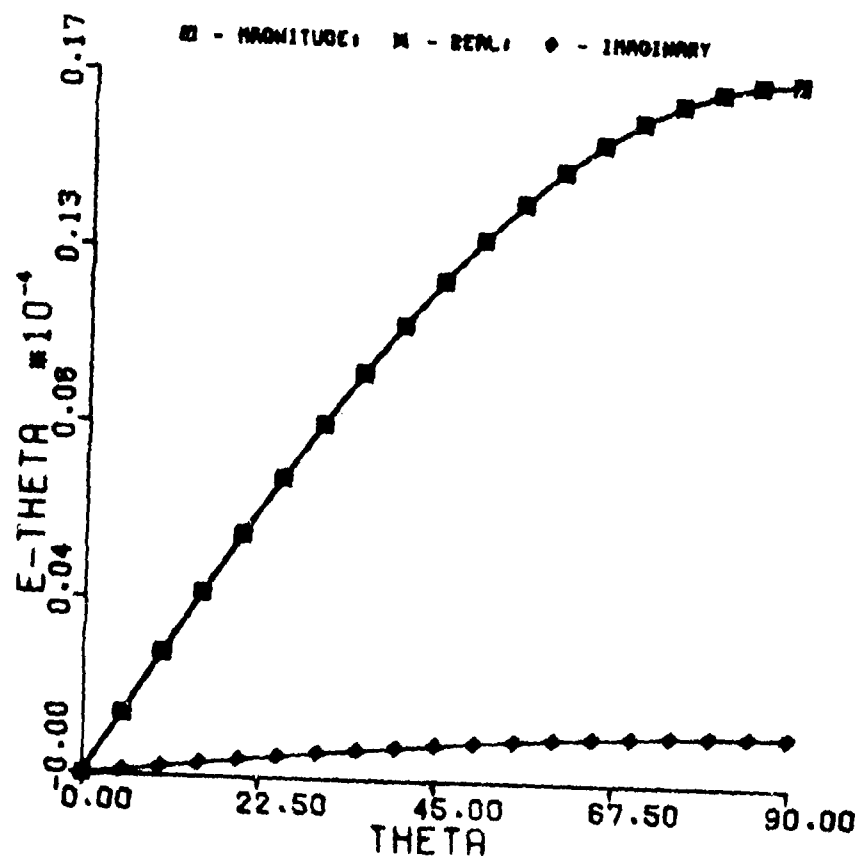


Figure 22.  $E_\theta$  radiation pattern for loaded cone with topcap,  $L=54.05\text{m}$ ,  $\theta = 42.26^\circ$ ,  $V_0 = 1 \text{ Volt}$ ,  $f = 550 \text{ KHz}$ ,  $r = 10^4\text{m}$ .

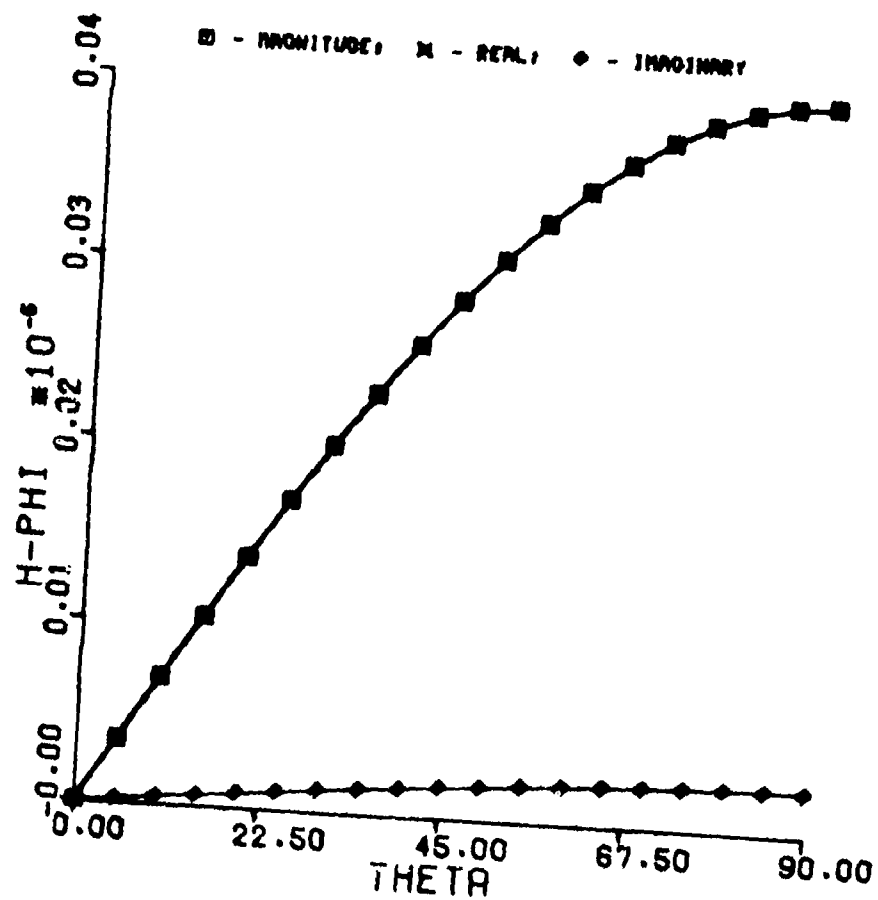


Figure 23.  $H_0$  radiation pattern for loaded cone with topcap,  $L=54.05m$ ,  $\theta_0 = 42.26^\circ$ ,  $V_0 = 1$  Volt,  $f = 550$  KHz,  $r = 10^4m$ .

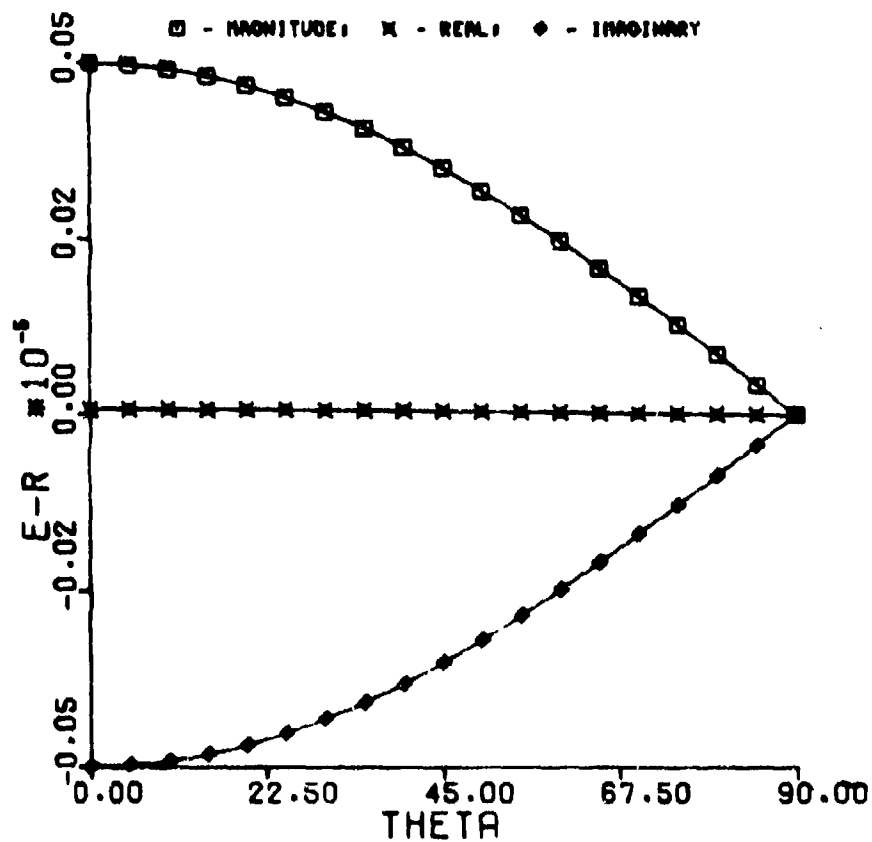


Figure 24.  $E_r$  radiation pattern for loaded cone with topcap,  $L=54.05m$ ,  $\theta_0 = 42.26^\circ$ ,  $V_0 = 1$  Volt,  $f = 550$  KHz,  $r = 10^4m$ .

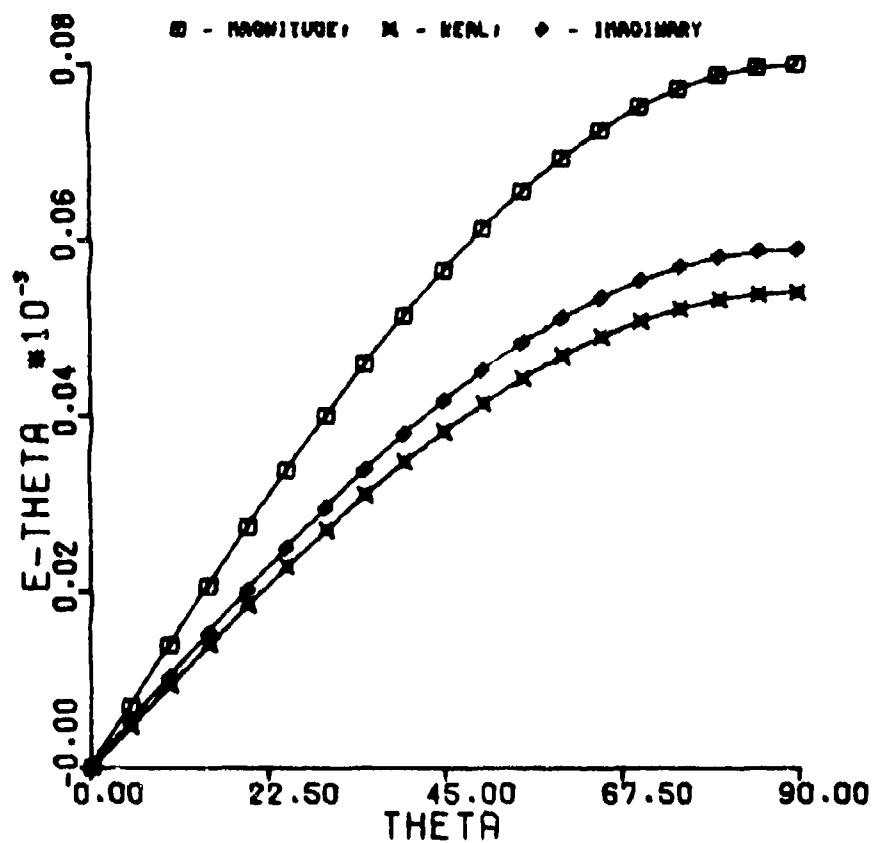


Figure 25.  $E_\theta$  radiation pattern for unloaded cone with topcap,  $L=54.05m$ ,  $\theta_0 = 42.26^\circ$ ,  $V_0 = 1$  Volt,  $f = 550$  KHz,  $r = 10^4m$ .

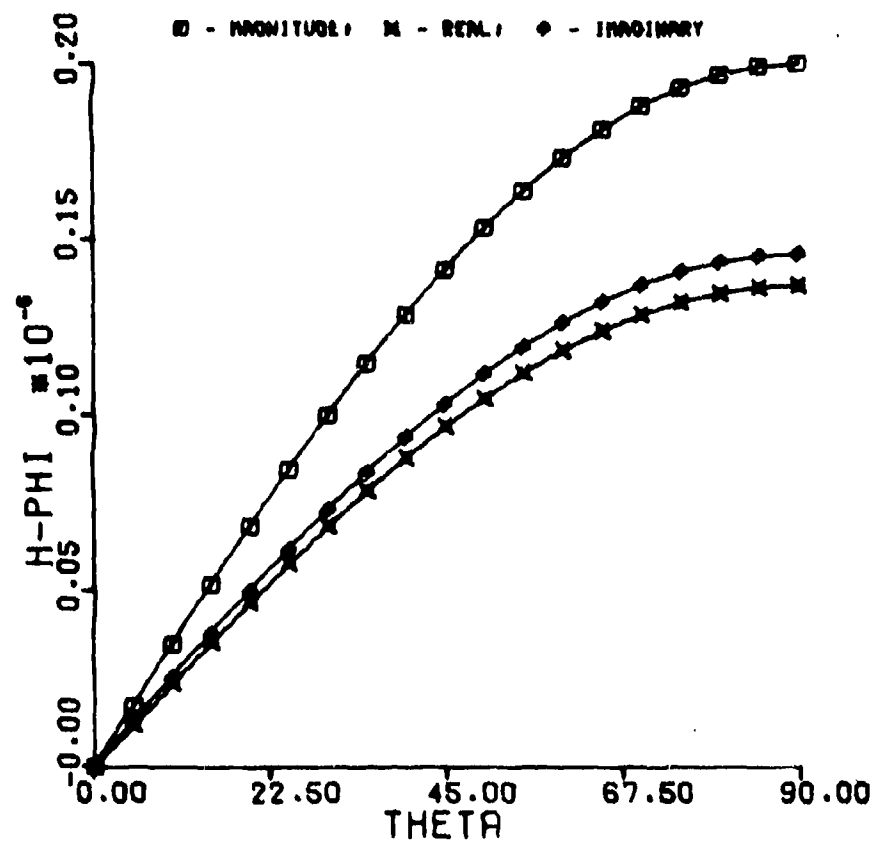


Figure 26.  $H_\phi$  radiation pattern for unloaded cone with topcap,  $L=54.05\text{m}$ ,  $\theta_0 = 42.26^\circ$ ,  $V_0 = 1 \text{ Volt}$ ,  $f = 550 \text{ KHz}$ ,  $r = 10^4 \text{ m}$ .

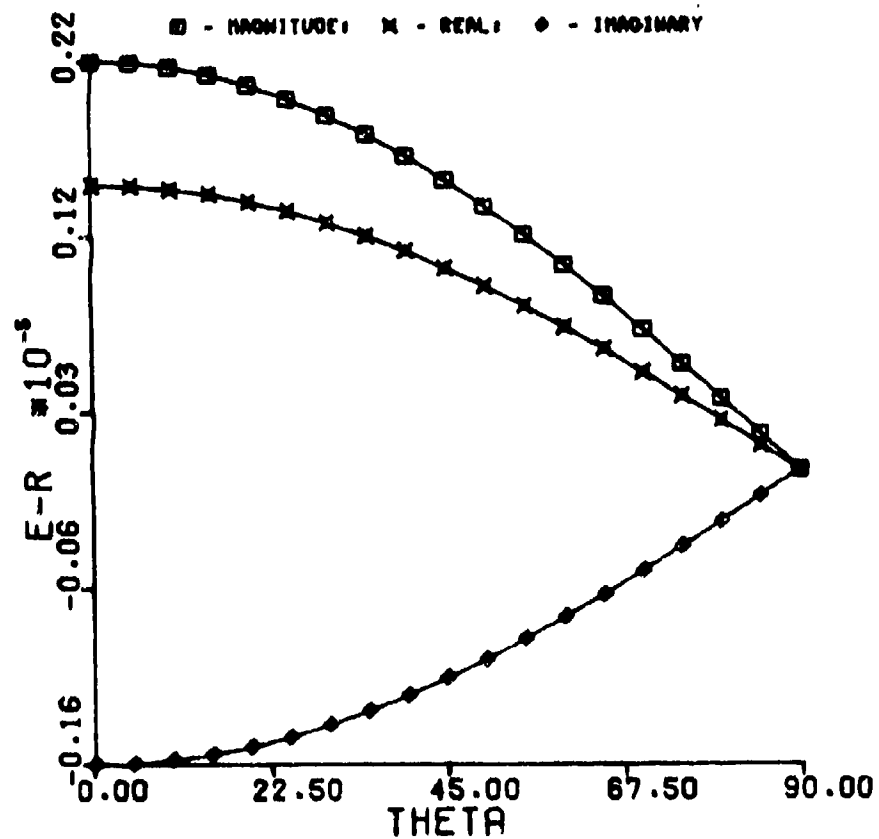


Figure 27.  $E_r$  radiation pattern for unloaded cone with topcap,  $L=54.05m$ ,  $\theta = 42.26^\circ$ ,  $V_0 = 1$  Volt,  $f = 550$  KHz,  $r = 10^4m$ .

ambitious project would more carefully model the actual wire structure with loading.

One conclusion of this and the companion study [1] is that the addition of a topcap does not significantly change the electromagnetic parameters of the structure - at low frequencies, the static capacitance and effective heights are almost unchanged and at the higher frequencies, the loading and the sharp angle at the edge tend to prevent current from flowing on the topcap. This observation may have some impact on the design of future simulators.



#### ACKNOWLEDGEMENT

The author gratefully acknowledges the able assistance of Mr. Allen Glisson in carrying out the computations.

## REFERENCES

1. D.R. Wilton, "Static Analysis of Conical Antenna over a Ground Plane," Final Report, Grant No. AFOSK 75-2832, Air Force Office of Scientific Research, Bolling Air Force Base, Washington, D.C., August, 1976.
2. R.F. Harrington, Time-Harmonic Electromagnetic Fields, McGraw-Hill, New York, 1961.
3. F.M. Tesche, A.R. Neureuther, and R.E. Stovall, "The Analysis of Monopole Antennas Located on a Spherical Vehicle," Interaction Note 198, Air Force Weapons Laboratory, Albuquerque, New Mexico, October, 1974.
4. R.F. Harrington, Field Computation by Moment Methods Macmillan, New York, 1968.
5. S.A. Scheikunoff, Electromagnetic Waves, Van Nostrand, Princeton, 1943.
6. W.S. Kehrter and C.E. Baum, "Electromagnetic Design Parameters for ATHAMAS II," ATHAMAS Memos, Memo No. 4, Air Force Weapons Laboratory, Albuquerque, New Mexico, May, 1975.
7. D.S. Jones, The Theory of Electromagnetism, Pergamon, London, 1964.

# APPENDIX A

## CALCULATION OF RADIATED FIELDS

Once numerical values for the current distribution have been determined, the fields radiated by the bicone structure can readily be determined. Because of the symmetry of the structure and the excitation, the only non-zero components of the electric and magnetic fields are  $E_r$ ,  $E_\theta$ , and  $H_\phi$ . These are defined in terms of the vector and scalar potentials as

$$E_r = -j\omega A_r - \frac{\partial \Phi}{\partial r}$$

$$E_\theta = -j\omega A_\theta - \frac{1}{r} \frac{\partial \Phi}{\partial \theta}$$

$$\mu H_\phi = \frac{1}{r} A_\theta + \frac{\partial A_\theta}{\partial r} - \frac{1}{r} \frac{\partial A_r}{\partial \theta} \quad (A-1)$$

where  $\bar{A} = A_r \hat{r} + A_\theta \hat{\theta}$ . A spherical coordinate system centered at the bicone feed and with  $\theta$  measured from the z-axis is assumed. Since the fields are  $\phi$ -independent, all fields are evaluated in the x-z plane where  $\phi = 0$ . The vector potential and scalar potential are given by

$$A_p(r, \theta) = \frac{\mu}{8\pi^2} \left\{ \frac{I_1}{2} \psi_{pc}(r, \theta, r_1 + \Delta r_c/4) \right. \\ \left. + \sum_{n=2}^{N_c} I_n \psi_{pc}(r, \theta, r_n) + \right.$$

$$\begin{aligned}
& + \frac{I_{N_c+1}}{2} \left[ \psi_{pc}(r, \theta, L - \frac{\Delta r_c}{4}) + \psi_{pt}(r, \theta, r_{N_c+1} - \frac{\Delta r_t}{4}) \right] \\
& + \sum_{n=N_c+2}^N I_n \psi_{pt}(r, \theta, r_n) \Bigg\}; \quad p = r, \theta
\end{aligned} \tag{A-2}$$

$$\begin{aligned}
\phi(r, \theta) = & \frac{-1}{8\pi^2 j \omega \epsilon} \left[ \sum_{n=1}^{N_c} \left( \frac{I_{n+1} - I_n}{\Delta r_c} \right) \psi_c \left( r, \theta, r_n + \frac{\Delta r_c}{2} \right) \right. \\
& \left. + \sum_{n=N_c+1}^N \left( \frac{I_{n+1} - I_n}{\Delta r_t} \right) \psi_t \left( r, \theta, r_n - \frac{\Delta r_t}{2} \right) \right]
\end{aligned} \tag{A-3}$$

where the currents and coordinates are defined in Section IV.

The potential functions  $\Psi$  and  $\psi$  are defined as

$$\Psi_{pq}(r, \theta, r_q) = \Delta r_q \int_0^{2\pi} \left( \cos \xi_{pq}^+ \frac{e^{-jkR_q^+}}{R_q^+} + \cos \xi_{pq}^- \frac{e^{-jkR_q^-}}{R_q^-} \right) d\phi' \tag{A-4}$$

$$\psi_q(r, \theta, r_q) = \Delta r_q \int_0^{2\pi} \left( \frac{e^{-jkR_q^+}}{R_q^+} - \frac{e^{-jkR_q^-}}{R_q^-} \right) d\phi', \quad p=r, \theta; \quad q=c, t \tag{A-5}$$

where

$$\cos \xi_{rc}^{\pm} = \pm \sin \theta \cos \phi' \sin \theta_0 + \cos \theta \cos \theta_0$$

$$\cos \xi_{\theta c}^{\pm} = \pm \cos \theta \cos \phi' \sin \theta_0 - \sin \theta \cos \theta_0$$

$$\cos \xi_{rt}^{\pm} = \mp \sin \theta \cos \phi'$$

$$\cos \xi_{\theta t}^{\pm} = \mp \cos \theta \cos \phi'$$

and the radius vectors are all of the form

$$R_q^{\pm} = \sqrt{r_q'^2 + 2b_q^{\pm} r_q' + c_q^{\pm}}$$

with

$$b_c^{\pm} = -r \cos \phi' \sin \theta \sin \theta_0 \mp r \cos \theta \cos \theta_0 - a \cot \theta_0$$

$$c_c^{\pm} = r^2 \pm 2ra \cos \theta \csc \theta_0 + a^2 \csc^2 \theta_0$$

$$b_t^{\pm} = -r \sin \theta \cos \phi'$$

$$c_t^{\pm} = r^2 \mp 2rL \cos \theta \cos \theta_0 + L^2$$

Assuming a suitable choice for  $\Delta r$  and  $\Delta \theta$ , one may approximately compute the fields in (A-1) by finite difference approximations;

$$E_r(r, \theta) = -j\omega A_r(r, \theta) - \frac{\Phi(r+\Delta r, \theta) - \Phi(r, \theta)}{\Delta r}$$

$$E_{\theta}(r, \theta) = -j\omega A_{\theta}(r, \theta) - \frac{\Phi(r, \theta+\Delta \theta) - \Phi(r, \theta)}{r\Delta \theta}$$

$$\mu H_{\phi} = \frac{1}{r} A_{\theta}(r, \theta) + \frac{A_{\theta}(r+\Delta r, \theta) - A_{\theta}(r, \theta)}{\Delta r}$$

$$- \frac{A_r(r, \theta+\Delta \theta) - A_r(r, \theta)}{r\Delta \theta}$$

(A-6)

APPENDIX B  
AN ALTERNATE INTEGRAL EQUATION FOR  
A CONE WITH TOPCAP

The purpose of this appendix is to show how a novel identity involving the free space Green's function may be used to change the integral equation into a form where the testing procedure of Section III is applicable. In exchange for simplicity in the form resulting from the testing procedure, however, one obtains extremely complicated kernels in the integral equation. Furthermore, the new kernels have a number of singularities other than the usual one where match points and field points coincide. These complications make both the analysis and the numerical treatment tedious. Nevertheless, numerical results have been obtained for several cases using the approach and the results are in good agreement with data obtained by the method of Section III. For simplicity, we treat here only the unloaded cone.

As a prelude to the integral equation derivation, we derive a transformation of the formula for electric field components. Consider the x-component of electric field given by

$$\begin{aligned} j\omega\mu E_x &= \hat{x} \cdot (k^2 + \nabla\nabla \cdot) \bar{A} \\ &= k^2 A_x + \frac{\partial}{\partial x} (\nabla \cdot \bar{A}) \\ &= \left( \frac{\partial^2}{\partial x^2} + k^2 \right) A_x + \frac{\partial^2 A_y}{\partial x \partial y} + \frac{\partial^2 A_z}{\partial x \partial z} \end{aligned} \quad (B-1)$$

where the vector potential  $\bar{A}$  in terms of current density

$\bar{J}$  is

$$\bar{A} = \frac{\mu}{4\pi} \int_V \bar{J} \frac{e^{-jk|\bar{r}-\bar{r}'|}}{|\bar{r}-\bar{r}'|} dV' \quad (B-2)$$

The identity

$$\frac{\partial^2}{\partial u \partial v} \left( \frac{e^{-jkR}}{R} \right) = - \left( \frac{\partial^2}{\partial u^2} + k^2 \right) \left[ \frac{uv}{v^2+w^2} \left( \frac{e^{-jkR}}{R} \right) \right] \quad (B-3)$$

where  $R = \sqrt{u^2+v^2+w^2}$  can be used with  $u = x-x'$ ,  $v = y-y'$ , and  $w = z-z'$  to rewrite (B-1) as

$$\begin{aligned} j\omega\mu\epsilon E_x &= \left( \frac{\partial^2}{\partial x^2} + k^2 \right) \int_V \left( J_x - J_y \frac{(x-x')(y-y')}{(y-y')^2+(z-z')^2} \right. \\ &\quad \left. - J_z \frac{(x-x')(z-z')}{(y-y')^2+(z-z')^2} \right) \frac{e^{-jkR}}{R} dV' \\ &= \left( \frac{\partial^2}{\partial x^2} + k^2 \right) \int_V \left( \bar{J} \cdot \hat{x} - \frac{(x-x')[\hat{y}(y-y')+\hat{z}(z-z')]}{(y-y')^2+(z-z')^2} \right) \\ &\quad \times \frac{e^{-jkR}}{R} dV' \quad (B-4) \end{aligned}$$

The vector  $\bar{r}-\bar{r}' = (x-x')\hat{x} + (y-y')\hat{y} + (z-z')\hat{z}$  can be written as the sum

$$\bar{r}-\bar{r}' = (\bar{r}-\bar{r}')_x \hat{x} + (\bar{r}-\bar{r}')_t \hat{t}$$

where

$$(\bar{r}-\bar{r}')_x = \hat{x} \cdot (\bar{r}-\bar{r}') = x-x'$$

is just the component of  $\bar{r}-\bar{r}'$  along the direction of  $\hat{x}$  and

$$(\bar{r}-\bar{r}')_t \hat{x} = \bar{r}-\bar{r}' - (\bar{r}-\bar{r}')_x \hat{x}$$

is just the component of  $\bar{r}-\bar{r}'$  transverse to  $\hat{x}$ . Thus,

(B-4) can be written as

$$j\omega\mu\epsilon E_x = \left(\frac{\partial^2}{\partial x^2} + k^2\right) \int_V \bar{J} \cdot \left( \hat{x} - \frac{\hat{x}(\bar{r}-\bar{r}')_t (\bar{r}-\bar{r}')_x}{(\bar{r}-\bar{r}')_t^2} \right) \frac{e^{-jkR}}{R} dV'$$

(B-5)

Since the choice of the coordinate system is arbitrary, we may choose the x-axis parallel to some constant unit vector  $\hat{a}$  and write the component of electric field in the direction of  $\hat{a}$  to be

$$\begin{aligned} j\omega\mu\epsilon E_a &= \left(\frac{\partial^2}{\partial s^2} + k^2\right) \int_V \bar{J} \cdot \left( \hat{a} - \frac{\hat{x}(\bar{r}-\bar{r}')_t (\bar{r}-\bar{r}')_x}{(\bar{r}-\bar{r}')_t^2} \right) \\ &\quad \times \frac{e^{-jkR}}{R} dV' \\ &= \left(\frac{\partial^2}{\partial s^2} + k^2\right) \int_V \bar{J} \cdot \left[ \hat{a} - \hat{x} \cot(\hat{a}, \bar{r}-\bar{r}') \right] \frac{e^{-jkR}}{R} dV' \end{aligned}$$

(B-6)

where now  $\hat{x}$  denotes the direction of the component of  $(\bar{r}-\bar{r}')$  transverse to  $\hat{a}$  and  $s$  denotes distance along a line in the direction of  $\hat{a}$ . Note that the integrand in (B-6) is singular not only when  $R=0$ , but also when the angle between  $\hat{a}$  and  $\bar{r}-\bar{r}'$  becomes either  $0^\circ$  or  $180^\circ$ . Since in (B-6) the



only differential operator is the harmonic operator, then along a line in the direction of  $\hat{a}$ , the testing procedure of Section III which uses piecewise sinusoids may again be used to transform the harmonic operator into a finite difference operator. This is the advantage, gained at the expense of obtaining a more complicated kernel, of employing the transformation (B-3).

Returning to the cone problem, we choose the direction of  $\hat{a}$  to be along the cone generator formed by the intersection of the  $\phi=0$  plane and the cone surface, and apply the boundary conditions. After some straightforward but tedious vector projection operations, one arrives at the integral equations

$$\frac{1}{j\omega\mu\epsilon} \left( \frac{\partial^2}{\partial r_c^2} + k^2 \right) \left( \psi_{cc} + \psi_{ct} \right) = -V_0 \delta(r_c - 0^+),$$

$$0 \leq r_c \leq L \quad (B-7)$$

$$\frac{1}{j\omega\mu\epsilon} \left( \frac{\partial^2}{\partial r_t^2} + k^2 \right) \left( \psi_{tc} + \psi_{tt} \right) = 0, \quad 0 \leq r_t \leq L \sin \theta_0 \quad (B-8)$$

where

$$\psi_{pc}(r_p) = \frac{\mu}{8\pi^2} \int_0^{2\pi} \int_0^L I_c(r'_c) (K_{pc}^+ + K_{pc}^-) dr'_c d\phi',$$

$$\psi_{pt}(r_p) = \frac{\mu}{8\pi^2} \int_0^{2\pi} \int_0^{L \sin \theta_0} I_t(r'_t) (K_{pt}^+ + K_{pt}^-) dr'_t d\phi',$$

$$p = c \text{ or } t \quad (B-9)$$

The kernels  $K_{pq}^{\pm}$  in (B-9) are of the form

$$K_{pq}^{\pm}(r_p, r'_q, \phi') = \left( D_{pq}^{\pm}(\phi') + \frac{C_{pq}^{\pm}(r'_q, \phi') [A_{pq}^{\pm}(\phi') r'_q + B_{pq}^{\pm}(\phi')] }{R_{pq}^{\pm 2} - C_{pq}^{\pm 2}(r'_q, \phi')} \right) \times \frac{e^{-jkR_{pq}^{\pm}}}{R_{pq}^{\pm}}$$

The distance between source points and field points,  $R_{pq}^{\pm}$ , is of the form

$$R_{pq}^{\pm} = \sqrt{r_q'^2 + 2b_{pq}^{\pm} r'_q + c_{pq}^{\pm}}$$

and  $b_{pq}^{\pm}$  and  $c_{pq}^{\pm}$  are as defined in Section IV with "a" set equal to zero. The term  $C_{pq}^{\pm}$  may be expressed as

$$C_{pq}^{\pm} = e_{pq}^{\pm} r'_q + f_{pq}^{\pm}$$

The parameters  $A_{pq}^{\pm}$ ,  $B_{pq}^{\pm}$ ,  $D_{pq}^{\pm}$ , and  $f_{pq}^{\pm}$  are defined in Tables (B-1)-(B-4).

Testing Equations (B-7) and (B-8) with piecewise - sinusoidal testing functions as in Section III results in the equations

$$\frac{k}{j\omega\mu\epsilon\sin k\Delta r_c} \left\{ -\cos k\Delta r_c [\Psi_{cc}(r_{c1}) + \Psi_{ct}(r_{c1})] + [\Psi_{cc}(r_{c2}) + \Psi_{ct}(r_{c2})] \right\} = -V_0 \quad (B-10)$$

TABLE B-1

DEFINITIONS OF PARAMETERS FOR THE KERNEL  $K_{cc}$ 

$$A_{cc}^{\pm} = \sin^2 \theta_0 [\sin^2 \phi' + \cos^2 \theta_0 (\cos \phi' \mp 1)^2]$$

$$B_{cc}^{\pm} = 0$$

$$D_{cc}^{\pm} = -e_{cc}^{\pm} = \sin^2 \theta_0 \cos \phi' \pm \cos^2 \theta_0$$

$$f_{cc}^{\pm} = r_c$$

TABLE B-2

DEFINITIONS OF PARAMETERS FOR THE KERNEL  $K_{ct}$ 

$$A_{ct}^{\pm} = \cos^2 \theta_0 \cos^2 \phi' + \sin^2 \phi'$$

$$B_{ct}^{\pm} = \mp L \cos^2 \theta_0 \sin \theta_0 \cos \phi'$$

$$D_{ct}^{\pm} = -e_{ct}^{\pm} = \sin \theta_0 \cos \phi'$$

$$f_{ct}^{\pm} = r_c \mp L \cos^2 \theta_0$$

TABLE B-3

DEFINITIONS OF PARAMETERS FOR THE KERNEL  $K_{tc}$ 

$$A_{tc}^{\pm} = \sin^2 \theta_0 \sin^2 \phi' \pm \cos^2 \theta_0$$

$$B_{tc}^{\pm} = -L \cos^2 \theta_0$$

$$D_{tc}^{\pm} = -e_{tc}^{\pm} = \sin \theta_0 \cos \phi'$$

$$f_{tc}^{\pm} = r_t$$

TABLE B-4

DEFINITIONS OF PARAMETERS FOR THE KERNEL  $K_{tt}$ 

$$A_{tt}^{\pm} = \sin^2 \phi'$$

$$B_{tt}^{\pm} = 0$$

$$D_{tt}^{\pm} = e_{tt}^{\pm} = \cos \phi'$$

$$f_{tt}^{\pm} = r_t$$

and

$$\begin{aligned} & \frac{k}{j\omega\mu\epsilon\sin k\Delta r_c} \left\{ [\Psi_{cc}(r_{c,m+1}) + \Psi_{ct}(r_{c,m+1})] \right. \\ & \quad - 2 \cos k\Delta r_c [\Psi_{cc}(r_{cm}) + \Psi_{ct}(r_{cm})] \\ & \quad \left. + [\Psi_{cc}(r_{c,m-1}) + \Psi_{ct}(r_{c,m-1})] \right\} = 0, \\ & \quad m=2,3,\dots,N_c-1 \end{aligned} \tag{B-11}$$

Testing at the cone edge with a piecewise sinusoidal testing function which straddles both the cone and the topcap and which has its peak value at the cone edge, one obtains

$$\begin{aligned} & \frac{k}{j\omega\mu\epsilon\sin k\Delta r_c} \left\{ - \cos k\Delta r_c [\Psi_{cc}(r_{cNc}) + \Psi_{ct}(r_{cNc})] \right. \\ & \quad \left. + [\Psi_{cc}(r_{c,N_c-1}) + \Psi_{ct}(r_{c,N_c-1})] \right\} \\ & + \frac{k}{j\omega\mu\epsilon\sin k\Delta r_t} \left\{ - \cos k\Delta r_t [\Psi_{tc}(r_{t1}) + \Psi_{tt}(r_{t1})] \right. \\ & \quad \left. + [\Psi_{tc}(r_{t2}) + \Psi_{tt}(r_{t2})] \right\} \\ & + \frac{1}{j\omega\mu\epsilon} \left\{ \left[ \frac{\partial \Psi_{cc}}{\partial r_c} + \frac{\partial \Psi_{ct}}{\partial r_c} \right]_{r_c=r_{cNc}} + \left[ \frac{\partial \Psi_{tc}}{\partial r_t} + \frac{\partial \Psi_{tt}}{\partial r_t} \right]_{r_t=r_{t1}} \right\} = 0 \end{aligned} \tag{B-12}$$

Finally, testing on the topcap surface yields

$$\begin{aligned} & \frac{k}{j\omega\mu\epsilon\sin k\Delta r_t} \left\{ [\Psi_{tc}(r_{t,m+1}) + \Psi_{tt}(r_{t,m+1})] \right. \\ & \quad \left. - 2 \cos k\Delta r_t [\Psi_{tc}(r_{tm}) + \Psi_{tt}(r_{tm})] + \right. \end{aligned}$$

$$+ [\Psi_{tc}(r_{t,m-1}) + \Psi_{tt}(r_{t,m-1})] \} = 0,$$

$$m=2,3,\dots,N_t+1 \quad (B-13)$$

Substitution of the current expansions, Eqs. (40) and (41) of Section IV, into (B-10)-(B-13) yields a matrix equation for the determination of the unknown current coefficients. Because of the pulse expansion for the current, the matrix elements involve integrals like (B-9) but with the current in (B-9) equal to unity and the limits on the radial integration replaced by the limits of the corresponding current subdomain. According to (B-12), the term at the edge also requires the derivative of such integrals. In the following, we present a procedure for approximately evaluating the radial integration, leaving the  $\phi'$  integration to be done numerically. The required integrals are all of the form

$$\int_{r_{n-}}^{r_{n+}} K dr' = \int_{r_{n-}}^{r_{n+}} \left[ D + \frac{C(Ar' + B)}{R^2 - C^2} \right] \frac{e^{-jkR}}{R} dr' \quad (B-14)$$

where, for convenience, all subscripts and superscripts have been suppressed. Since the number of subdomains should be chosen such that  $k|r_{n+} - r_{n-}|$  is small, we chose some point  $r_n$  in the interval  $[r_{n+}, r_{n-}]$  and expand  $\exp(-jkR)$  in a Taylor series about the point  $r' = r_n$ ;

$$\begin{aligned}
 e^{-jkR} &= e^{-jkR_n} e^{-jk(R-R_n)} \\
 &\approx e^{-jkR_n} [1 - jk(R-R_n)] \quad (B-15)
 \end{aligned}$$

where  $R_n$  denotes  $R$  evaluated at  $r'=r_n$ . The resulting approximate integral is

$$\begin{aligned}
 \int_{r_{n-}}^{r_{n+}} K \, dr' &\approx e^{-jkR_n} \int_{r_{n-}}^{r_{n+}} \left[ D + \frac{C(Ar'+B)}{R^2-C^2} \right] \left[ \frac{1-jk(R-R_n)}{R} \right] dr' \\
 &= e^{-jkR_n} (I_1 + I_2 + I_3) \quad (B-16)
 \end{aligned}$$

where

$$I_1 = -jk \int_{r_{n-}}^{r_{n+}} \left( D + \frac{C(Ar'+B)}{R^2-C^2} \right) dr'$$

$$I_2 = D(1+jkR_n) \int_{r_{n-}}^{r_{n+}} \frac{dr'}{R}$$

and

$$I_3 = (1+jkR_n) \int_{r_{n-}}^{r_{n+}} \frac{C(Ar'+B)}{R^2-C^2} \frac{dr'}{R}$$

The first integral may be evaluated by substituting the definitions for  $R$  and  $C$  in terms of  $b, c, e$ , and  $f$ ;

$$\begin{aligned}
I_1 &= -jk \int_{r_{n-}}^{r_{n+}} \left( D + \frac{Ae r'^2 + (Be + Af) r' + Bf}{(1-e^2) r'^2 + 2(b-ef) r' + c-f^2} \right) dr' \\
&= -jk \left\{ F_1 (r_{n+} - r_{n-}) + F_2 \ln \left| \frac{R_{n+}^2 - C_{n+}^2}{R_{n-}^2 - C_{n-}^2} \right| \right. \\
&\quad + F_3 \left[ \tan^{-1} \left( \frac{(1-e^2) r_{n+} + (b-ef)}{\sqrt{(1-e^2)(c-f^2) - (b-ef)^2}} \right) \right. \\
&\quad \left. \left. - \tan^{-1} \left( \frac{(1-e^2) r_{n-} + (b-ef)}{\sqrt{(1-e^2)(c-f^2) - (b-ef)^2}} \right) \right] \right\} \quad (B-17)
\end{aligned}$$

where

$$F_1 = D + \frac{Ae}{1-e^2}$$

$$F_2 = \frac{(Be + Af)(1-e^2) - 2Ae(b-ef)}{2(1-e^2)^2}$$

$$\begin{aligned}
F_3 &= [2Ae(b-ef)^2 - Ae(1-e^2)(c-f^2) - (Be + Af)(b-ef)(1-e^2) + Bf(1-e^2)^2] \\
&\quad \times [(1-e^2)^2 \sqrt{(1-e^2)(c-f^2) - (b-ef)^2}]^{-1}
\end{aligned}$$

The tabulated integrals Dw 160.01, 160.11, and 160.21 aid in the evaluation of  $I_1$ <sup>†</sup>.  $I_2$  may be evaluated using Dw. 380.001 as

$$I_2 = D(1 + jkR_n) \int_{r_{n-}}^{r_{n+}} \frac{dr'}{R}$$

<sup>†</sup>The abbreviations Dw and GR refer to Tables of Integrals and other Mathematical Data, Fourth Ed., H.B. Dwight, Macmillan, N.Y., 1961; and Tables of Integrals, Series and Products, I.S. Gradshteyn and I.W. Ryshik, Academic Press, N.Y., 1965, respectively.



$$= D(1+jkR_n) \ln \frac{R_{n+} + r_{n+} + b}{R_{n-} + r_{n-} + b} \quad (B-18)$$

The subscripts  $n$ ,  $n+$ , and  $n-$  denote quantities which are evaluated at  $r'=r_n$ ,  $r_{n+}$ , and  $r_{n-}$ , respectively.

The evaluation of  $I_3$  is facilitated by expanding it in partial fractions and using the substitution  $\sinh \theta = (r'+b)/\sqrt{c-b^2}$  to obtain

$$\begin{aligned} I_3 &= (1+jkR_n) \int_{r_{n-}}^{r_{n+}} \frac{C(Ar'+B)}{R^2-C^2} dr' \\ &= \frac{(1+jkR_n)}{2} \int_{r_{n-}}^{r_{n+}} \left( \frac{1}{R-C} - \frac{1}{R+C} \right) \frac{(Ar'+B)}{R} dr' \\ &= \frac{(1+jkR_n)}{2} \int_{\theta_{n-}}^{\theta_{n+}} (A\sqrt{c-b^2} \sinh \theta + B-Ab) \\ &\quad \times \left( \frac{1}{\sqrt{c-b^2} \cosh \theta - e^{\sqrt{c-b^2} \sinh \theta} - f+be} \right. \\ &\quad \left. - \frac{1}{\sqrt{c-b^2} \cosh \theta + e^{\sqrt{c-b^2} \sinh \theta} + f-be} \right) d\theta \end{aligned}$$

Using GR 2.451.2 and GR 2.451.4, one finds the latter integral to be

$$\begin{aligned}
I_3 = & (1+jkR_n) \left[ \frac{Ae}{1-e^2} \ell_n \left| \frac{R_{n+}+r_{n+}+b}{R_{n-}+r_{n-}+b} \right| \right. \\
& + \frac{A}{2(1-e^2)} \ell_n \left| \frac{(R_{n+}-C_{n+})(R_{n-}+C_{n-})}{(R_{n-}-C_{n-})(R_{n+}+C_{n+})} \right| \\
& + F_4 \left[ \tan^{-1} \frac{\sqrt{c-b^2}(R_{n-}-C_{n-})-(be-f)R_{n+}+b^2-c}{F_5(r_{n+}+b)} \right. \\
& - \tan^{-1} \frac{\sqrt{c-b^2}(R_{n-}-C_{n-})-(be-f)R_{n-}+b^2-c}{F_5(r_{n-}+b)} \\
& - \tan^{-1} \frac{\sqrt{c-b^2}(R_{n+}+C_{n+})+(be-f)R_{n+}+b^2-c}{F_5(r_{n+}+b)} \\
& \left. \left. + \tan^{-1} \frac{\sqrt{c-b^2}(R_{n-}+C_{n-})+(be-f)R_{n-}+b^2-c}{F_5(r_{n-}+b)} \right] \right] \quad (B-19)
\end{aligned}$$

where

$$F_4 = \frac{(B-Ab)(1-e^2)-Ae(be-f)}{F_5(1-e^2)}$$

$$F_5 = \sqrt{(c-b^2(1-e^2)-(be-f)^2)}$$

Equations (B-17)-(B-19) complete the evaluation of (B-16).

The derivative terms appearing in (B-12) require evaluation of integrals of the form

$$\frac{\partial}{\partial r} \int_{r_{n-}}^{r_{n+}} K dr' = \frac{\partial}{\partial r} \int_{r_{n-}}^{r_{n+}} \left[ D + \frac{C(Ar+B)}{R^2-C^2} \right] \frac{e^{-jkR}}{R} dr' \quad (B-20)$$

where the unprimed variable  $r$  is  $r_c$  or  $r_t$ , as appropriate. The two edge terms also have non-integrable singularities at the edge which cancel between the various terms. To handle this situation numerically, the singularity must be explicitly identified and removed for numerical integration. Thus the same kind of approximate analytical integration of (B-20) as used to evaluate (B-16) would both eliminate one integration and explicitly identify the singular term. The derivative can be taken inside the integral if care is taken to identify the singular terms. Noting that  $\partial C/\partial r = 1$ ,  $\partial(R^2 - C^2)/\partial r = 0$ , and  $\partial A/\partial r = \partial B/\partial r = 0$ , we have

$$\begin{aligned} \frac{\partial}{\partial r} \int_{r_{n-}}^{r_{n+}} K \, dr' &= \int_{r_{n-}}^{r_{n+}} \left[ -\frac{j k D C}{R^2} - \frac{D C}{R^3} \right. \\ &\quad \left. + \frac{A r' + B}{R^2 - C^2} \left( \frac{1}{R} - \frac{j k C^2}{R^2} - \frac{C^2}{R^3} \right) \right] e^{-j k R} \, dr' \end{aligned}$$

With the approximation of (B-15), the above may be written as

$$\int_{r_{n-}}^{r_{n+}} \frac{\partial K}{\partial r} \, dr' \approx e^{-j k R_n} (I_4 + I_3 + I_6 + I_7 + I_8) \quad (\text{B-21})$$

The various integrals appearing in (B-21) are defined and evaluated as follows:

$$\begin{aligned}
I_4 &= -k^2 \int_{r_{n-}}^{r_{n+}} \frac{CD}{R} dr' = -k^2 \int_{r_{n-}}^{r_{n+}} \frac{D(er'+f)}{R} dr' \\
&= -k^2 \left[ De(R_{n+} - R_{n-}) - (be-f) \ln \left| \frac{R_{n+} + r_{n+} + b}{R_{n-} + r_{n-} + b} \right| \right] \quad (B-22)
\end{aligned}$$

where Dw 380.001 and Dw 380.011 have been used.

$$\begin{aligned}
I_5 &= k^2 R_n \int_{r_{n-}}^{r_{n+}} \frac{(De-A)r' + fD-B}{r'^2 + 2br' + c} dr' \\
&= k^2 R_n \left[ (De-A) \ln \left| \frac{R_{n+}}{R_{n-}} \right| \right. \\
&\quad \left. + \frac{fD-B-b(De-A)}{\sqrt{c-b^2}} \left( \tan^{-1} \frac{r_{n+}+b}{\sqrt{c-b^2}} - \tan^{-1} \frac{r_{n-}+b}{\sqrt{c-b^2}} \right) \right] \quad (B-23)
\end{aligned}$$

where Dw 160.01 and Dw 160.11 have been used. Using Dw 300.003 and Dw 380.013, one obtains

$$\begin{aligned}
I_6 &= (1+jkR_n) \int_{r_{n-}}^{r_{n+}} \frac{(A-De)r' + (B-Df)}{R^3} dr' \\
&= \frac{1+jkR_n}{c-b^2} \left\{ [B-Df-b(A-De)] \left( \frac{r_{n+}}{R_{n+}} - \frac{r_{n-}}{R_{n-}} \right) \right. \\
&\quad \left. + [b(B-Df)-c(A-De)] \left( \frac{1}{R_{n+}} - \frac{1}{R_{n-}} \right) \right\} \quad (B-24)
\end{aligned}$$

Again using Dw 160.01 and Dw 160.11, we have

$$\begin{aligned}
 I_7 &= -jk(1+jkR_n) \int_{r_{n-}}^{r_{n+}} \frac{Ar'+B}{R^2-C^2} dr' \\
 &= -jk(1+jkR_n) \int_{r_{n-}}^{r_{n+}} \frac{Ar'+B}{(1-e^2)r'^2+2(b-ef)r'+c-f^2} dr' \\
 &= -jk(1+jkR_n) \left\{ \frac{A}{2(1-e^2)} \ln \left| \frac{R_{n+}^2-C_{n+}^2}{R_{n-}^2-C_{n-}^2} \right| \right. \\
 &\quad \left. + \frac{B(1-e^2)-(b-ef)A}{(1-e^2)F_6} \left[ \tan^{-1} \left( \frac{(1-e^2)r_{n+}+b-ef}{F_6} \right) \right. \right. \\
 &\quad \left. \left. - \tan^{-1} \left( \frac{(1-e^2)r_{n-}+b-ef}{F_6} \right) \right] \right\}
 \end{aligned}$$

(B-25)

where

$$F_6 = \sqrt{(1-e^2)(c-f^2)-(b-ef)^2}$$

The remaining integral is

$$\begin{aligned}
 I_8 &= k^2 \int_{r_{n-}}^{r_{n+}} (Ar'+B) \left( \frac{1}{R} - \frac{R}{R^2-C^2} \right) dr' \\
 &= -k^2 \int_{r_{n-}}^{r_{n+}} \frac{C^2(Ar'+B)}{R(R^2-C^2)} dr'
 \end{aligned}$$

$$= -k^2 \int_{r_{n-}}^{r_{n+}} \frac{C(er' + f)(Ar' + B)}{R(R^2 - C^2)} dr'$$

$$= -k^2 \int_{r_{n-}}^{r_{n+}} \frac{C[Aer'^2 + (Af + Be)r' + Bf]}{R(R^2 - C^2)} dr'$$

Dividing  $R^2 - C^2 = (1 - e^2)r'^2 + 2(b - ef)r' + c - f^2$  into the bracketed term in the numerator of the integrand, we may write the integral as

$$I_8 = -k^2 \int_{r_{n-}}^{r_{n+}} \frac{C}{R} \left[ \frac{Ae}{1 - e^2} + \frac{(Af + Be + W)r' + Bf + U}{R^2 - C^2} \right] dr'$$

where

$$W = - \frac{2Ae(b - ef)}{1 - e^2}$$

$$U = - \frac{Ae(c - f^2)}{1 - e^2}$$

Expanding the second term in brackets in the integrand in partial fractions, one can write  $I_8$  as

$$I_8 = I_8' + I_8''$$

where

$$I_8' = \frac{-k^2 Ae}{1 - e^2} \int_{r_{n-}}^{r_{n+}} \frac{er' + f}{R} dr'$$

$$= \frac{-k^2 Ae}{1 - e^2} \left[ e(R_{n+} - R_{n-}) + (f - be) \ln \left| \frac{R_{n+} + r_{n+} + b}{R_{n-} + r_{n-} + b} \right| \right]$$

and

$$I_8'' = \frac{-k^2}{2} \int_{r_{n-}}^{r_{n+}} [(Af+Be+W)r' + Bf+U] \left( \frac{1}{R-C} - \frac{1}{R+C} \right) \frac{dr'}{R}$$

The substitution  $\sinh \theta = (r' + b)/\sqrt{c-b^2}$  enables one to write

$I_8''$  as

$$I_8'' = \frac{-k^2}{2} \int_{\theta_{n-}}^{\theta_{n+}} [ (Af+Be+W)\sqrt{c-b^2} \sinh \theta + Bf+U-b(Af+Be+W) ] \\ \times \left( \frac{1}{\sqrt{c-b^2} \cosh \theta - e^{\sqrt{c-b^2} \sinh \theta - f + be}} - \frac{1}{\sqrt{c-b^2} \cosh \theta + e^{\sqrt{c-b^2} \sinh \theta + f - be}} \right) dr'$$

Using GR 2.451.2 and GR 2.451.4, we obtain finally

$$I_8'' = -k^2 \left\{ \frac{Af+Be+W}{2(1-e^2)} \ln \left| \frac{(R_{n+}-C_{n+})(R_{n-}+C_{n-})}{(R_{n-}-C_{n-})(R_{n+}+C_{n+})} \right| \right. \\ \left. + \frac{e(Af+Be+W)}{(1-e^2)} \ln \left| \frac{R_{n+}+r_{n+}+b}{R_{n-}+r_{n-}+b} \right| \right. \\ \left. + F_7 \left[ \tan^{-1} \left( \frac{\sqrt{c-b^2}(R_{n+}-C_{n+}) - (be-f)R_{n+}+b^2-c}{(r_{n+}+b)F_5} \right) \right. \right. \\ \left. \left. - \tan^{-1} \left( \frac{\sqrt{c-b^2}(R_{n-}-C_{n-}) - (be-f)R_{n-}+b^2-c}{(r_{n-}+b)F_5} \right) \right] \right\}$$

$$\begin{aligned}
& - \tan^{-1} \left[ \frac{\sqrt{c-b^2}(R_{n+}+C_{n+}) + (be-f)R_{n+}+b^2-c}{(r_{n+}+b)F_5} \right] \\
& + \tan^{-1} \left[ \frac{\sqrt{c-b^2}(R_{n-}+C_{n-}) + (be-f)R_{n-}+b^2-c}{(r_{n-}+b)F_5} \right] \Bigg\} \quad (B-27)
\end{aligned}$$

where

$$F_7 = \frac{[Bf+U-b(Af+Be+W)](1-e^2)-e(be-f)(Af+Be+W)}{(1-e^2)F_5}$$

Equations (B-22) through (B-27) complete the evaluation of the integral, (B-21). Recall that the integral (B-21) needs to be evaluated only for observation points at the bicone edge (see Eq. (B-12)). For the source current pulse associated with the bicone edge, there results a non-integrable singularity (with respect to  $\phi'$  integration) which comes from the term  $1/R_{n+}$  in (B-24). Each of the derivative terms in (B-12) contains such a non-integrable singularity, however, and they are of opposite signs so as to cancel each other. For numerical integration, of course, the canceling singularities must be analytically subtracted.

The integrals  $I_1$  through  $I_8$  contain integrable singularities such as the usual one where source and field points coincide (i.e.,  $R=0$ ). In addition, however, there are also integrable singularities introduced by the transformation (B-6). These arise from current sources which lie along and are directed transverse to the line which passes through the observation point and which is in the direction of the



electric field component of interest. For example, in computing the tangential field component  $E_{r_c}$  on the cone, singularities arise from currents on the topcap and its image. While the many singularities complicate the numerical procedure, they can, in principle, be handled. However, the unwieldiness of the functions appearing in the integrals  $I_1$  through  $I_8$  makes the numerical procedure rather inefficient and subject to error. For example, the computer code derived from the formulation presented here seemed to yield reasonable results for moderate cone angles, but often yielded erroneous results for the very small cone angles used to check the program. The complexity of the formulation became a considerable hinderance in determining the source of these difficulties. Consequently, the final calculations were done using the formulation of Section III which was developed as an extension of methods currently being used to treat flat plate surfaces.